Eur. Phys. J. E (2005)
DOI 10.1140/epje/i2004-10088-x

THE EUROPEAN PHYSICAL JOURNAL E

Activated dynamics of semiflexible polymers on structured substrates

P. Kraikivski, R. Lipowsky, and J. Kierfeld[a]

Max-Planck-Institut für Kolloid- und Grenzflächenforschung, 14424 Potsdam, Germany

Received 16 July 2004 /
Published online: 28 January 2005 –

Abstract. We study the thermally activated motion of semiflexible polymers in double-well potentials using field-theoretic methods. Shape, energy, and effective diffusion constant of kink excitations are calculated, and their dependence on the bending rigidity of the semiflexible polymer is determined. For symmetric potentials, the kink motion is purely diffusive whereas kink motion becomes directed in the presence of a driving force. We determine the average velocity of the semiflexible polymer based on the kink dynamics. The Kramers escape over the potential barriers proceeds by nucleation and diffusive motion of kink-antikink pairs, the relaxation to the straight configuration by annihilation of kink-antikink pairs. We consider both uniform and point-like driving forces. For the case of point-like forces the polymer crosses the potential barrier only if the force exceeds a critical value. Our results apply to the activated motion of biopolymers such as DNA and actin filaments or of synthetic polyelectrolytes on structured substrates.

PACS. 82.35.Gh Polymers on surfaces; adhesion – 87.15.-v Biomolecules: structure and physical properties – 87.15.He Dynamics and conformational changes – 87.15.Tt Electrophoresis

1 Introduction

The problem of thermally activated escape of an object over a potential barrier is one of the central problems of stochastic dynamics since it has been first solved for a point particle by Kramers [1]. The Kramers problem is encountered in a variety of different areas such as the theory of diffusion in solids or chemical kinetics, such as the adhesion-kinetics of molecular bonds under a time-independent force [2]. The Kramers problem has been extensively studied not only for point particles [3] but also for extended objects such as elastic strings which occur in a variety of contexts in condensed-matter physics such as dislocation motion in crystals [4–7], motion of flux lines in type-II superconductors [8], or charge-density waves [9]. Elastic strings overcome potential barriers by nucleation and subsequent separation of soliton-antisoliton pairs which are localized kink excitations [5–7, 10,11]. An analogous problem is the activated motion of a flexible polymer over a potential barrier [12] which is relevant for biological processes such as the driven translocation of a polymer through a pore in a membrane [13].

However, the thermally activated escape of a semiflexible polymer, which is a filament governed by its bending energy rather than by its entropic elasticity or tension, remained an open question that we will address in this paper. Many important biopolymers such as DNA or actin filaments are semiflexible. They have a large bending stiffness and, thus, a large persistence length, L_p. On scales exceeding L_p, the orientational order of the polymer segments decays exponentially, and the polymer effectively behaves as a flexible chain with a segment size set by L_p. In contrast, on length scales which are small compared to L_p, the bending energy of the semiflexible polymer strongly affects the behaviour of the polymer. The persistence lengths of the most prominent biopolymers range from 50 nm for DNA [14], to the 10 μm range for actin [15,16] or even up to the mm range for microtubules [15] and become comparable to typical contour lengths of these polymers. Whereas the adsorption of such semiflexible polymers onto homogeneous adhesive surfaces has been studied previously in [17–19], much less is known about the behaviour of a semiflexible polymer adsorbed on a *structured* surface.

One example of semiflexible polymers on a chemically structured surface are long-chain alkanes and alkylated small molecules that self-assemble on crystalline substrates such as the basal plane of graphite [20] or transition metal dichalcogenides [21]. The alkyl chains orient along the substrate axes parallel to each other. Macromolecules such as DNA or polyelectrolytes can be oriented on the basal plane of graphite by using long-chain alkanes as an oriented template layer [22,23]. An important aspect is the ability to manipulate macromolecules individually on the structured surface by scanning probe techniques [23].

[a] e-mail: kierfeld@mpikg-golm.mpg.de

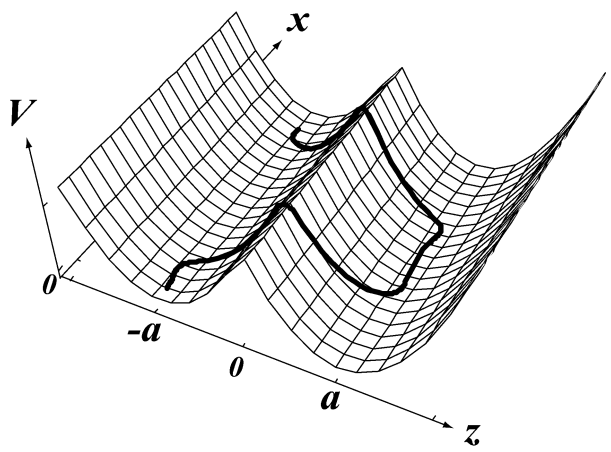

Fig. 1. Typical conformation of a semiflexible polymer (thick line) with a kink-antikink pair in a double-well potential V which depends on the coordinate z and is independent of the coordinate x.

Lithographically structured surfaces are used in electrophoresis [24] or microfluidic applications, where semiflexible biopolymers, such as actin filaments, can be deposited in microfluidic channels [25]. In electrophoresis applications lithographic barriers give rise to entropic free-energy barriers for the polymer. For the electrophoresis of semiflexible polymers, it is necessary to characterize the activated dynamics which leads to the crossing of such barriers. In particular, the dependence of the crossing time on the length of the semiflexible polymer determines the sensitivity of the process.

In this article, we focus on the activated dynamics of semiflexible polymers on a structured substrate with translationally invariant potential barriers as shown in Figure 1, which serves as model system for a chemically or lithographically structured surface. The activated dynamics can be driven by a variety of different force types. In this article, we mainly consider uniform driving forces across the potential barriers as they can be easily realized on structured substrates by electric fields for charged polymers as in electrophoresis or by hydrodynamic flow. Point-like driving forces can be realized in single molecule manipulation by AFM tips [23]. For point forces we consider static metastable configurations in this article; a complete description of the activated dynamics will be presented elsewhere. Alternatively, escape over a barrier can be driven by entropic forces arising from asymmetric shapes of the potential wells [26].

Our main results are as follows. As for flexible polymers, the activated dynamics of semiflexible polymers is governed by the nucleation of localized kink-like excitations shown in Figure 1. We find, however, that the activated dynamics of semiflexible polymers is different from that of flexible polymers as kink properties are not governed by entropic elasticity of the polymer chain but rather by the bending energy of the semiflexible polymer. This enables us to *determine the persistence length from kink properties*. Furthermore, we calculate time scales for barrier crossing and the mean velocity of the semiflexible polymer for all regimes of uniform driving forces: i) nucleation and purely diffusive motion of single kinks, ii) nucleation and driven diffusive motion of single kinks and iii) dynamic equilibria between nucleation and recombination in a kink ensemble. We not only consider uniform driving forces but also study metastable kink configurations if the force is only applied at a single point.

The paper is organized as follows: in Section 2, we introduce the model for a semiflexible polymer in 1+1 dimensions and its overdamped dynamics. A scaling analysis gives a characteristic energy, a characteristic length, a characteristic time scale and a characteristic velocity in the x-direction parallel to the potential troughs. In Section 3, we introduce a static kink. The shape and energy of the static kink are calculated. We also study the stability of kink-antikink pairs in Section 4. Then, we consider the motion of kinks in Sections 5, 6, and 7. The width of the moving kink and the force-velocity relation for a moving kink are calculated. We study in detail the effect of thermal noise on the kink motion and describe its diffusive motion. We calculate the effective diffusion constant of the kink excitation and find the relaxation or annihilation times for kink-antikink pairs. The thermally activated barrier crossing of the semiflexible polymer is governed by the nucleation of a kink-antikink pair as discussed in Section 9. We determine activation energy and nucleation rate. Using the results for the nucleation rate, we calculate the mean velocity of a polymer in the direction of the driving force in Section 10. In Section 11, we consider the effects of an external point force as opposed to a uniform force and calculate static, metastable kink-like configurations and the critical force. Finally, we discuss experimental observables and how they can be used to obtain material parameters of the polymer and the structured substrate in Section 12. A list of symbols is provided in Table 1. A short account of this work has already appeared as a letter [27].

2 Model

We consider the dynamics of a semiflexible polymer in 1+1 dimensions in a double-well potential that is translationally invariant in one direction, say the x-axis as in Figure 1. The semiflexible polymer has bending rigidity κ and persistence length

$$L_p = \frac{2\kappa}{T}, \tag{1}$$

where T is the temperature in energy units. We focus on the regime where the potential is sufficiently strong and the bending rigidity or persistence length is sufficiently large so that the semiflexible polymer is oriented along the x-axis and can be parameterized by displacements $z(x)$ perpendicular to the x-axis with $-L/2 < x < L/2$, where L is the projected length of polymer. The effective

Hamiltonian of the semiflexible polymer is given by

$$\mathcal{H}\{z(x)\} = \int_{-L/2}^{L/2} \mathrm{d}x \left[\frac{\kappa}{2}\left(\partial_x^2 z\right)^2 + V(z)\right] , \qquad (2)$$

i.e., the sum of its bending and potential energy. We consider a piecewise harmonic double-well potential

$$V(z) = \frac{1}{2}V_0(|z| - a)^2 - Fz \qquad (3)$$

that is independent of x and thus translationally invariant in the x-direction, where V_0 is the depth of the potential wells and F an external driving force density that is acting *uniformly* on all polymer segments. For a vanishing driving force $F = 0$, the potential is symmetric and has a barrier height $V_0 a^2/2$, and the distance between the two minima is equal to $2a$. For $F > 0$ the potential becomes asymmetric and has two minima at $z^{\pm}_{\mathrm{min}} = \pm a + F/V_0$ as long as the force is below the critical force

$$F_c \equiv aV_0 . \qquad (4)$$

Above the critical force for $F > F_c$, only the minimum at $z = z^{+}_{\mathrm{min}}$ is left.

The parameters κ, V_0, and a define a characteristic energy scale E_{sc} and a characteristic length scale x_{sc} in the x-direction by

$$E_{\mathrm{sc}} \equiv a^2\kappa^{1/4}V_0^{3/4}, \qquad (5)$$

$$x_{\mathrm{sc}} \equiv (\kappa/V_0)^{1/4} . \qquad (6)$$

Using the rescaling $\bar{z} \equiv z/a$ and $\bar{x} \equiv x/x_{\mathrm{sc}}$, the effective Hamiltonian (2) can be written in the dimensionless form

$$\mathcal{H} = E_{\mathrm{sc}} \int_{L/x_{\mathrm{sc}}} \mathrm{d}\bar{x} \left[\frac{1}{2}\left(\partial_{\bar{x}}^2 \bar{z}\right)^2 + \frac{1}{2}\left(|\bar{z}| - 1\right)^2 - \frac{F}{F_c}\bar{z}\right] . \qquad (7)$$

We consider an overdamped dynamics of the semiflexible polymer which is governed by the equation of motion

$$\begin{aligned}\gamma\partial_t z &= -\frac{\delta\mathcal{H}}{\delta z} + \zeta(x,t) \\ &= -\kappa\partial_x^4 z - V'(z) + \zeta(x,t),\end{aligned} \qquad (8)$$

where γ is the damping constant and $\zeta(x,t)$ is a Gaussian-distributed thermal random force with $\langle\zeta\rangle = 0$ and the correlation function

$$\langle\zeta(x,t)\zeta(x',t')\rangle = 2\gamma T\delta(x - x')\delta(t - t') . \qquad (9)$$

The parameters in the equation of motion (8) define a characteristic time scale t_{sc} and a characteristic velocity scale v_{sc} in x-direction by

$$t_{\mathrm{sc}} \equiv \gamma/V_0 , \qquad (10)$$

$$v_{\mathrm{sc}} \equiv x_{\mathrm{sc}}/t_{\mathrm{sc}} = \kappa^{1/4}V_0^{3/4}/\gamma . \qquad (11)$$

Using the rescaled quantities $\bar{t} \equiv t/t_{\mathrm{sc}}$, $\bar{z} \equiv z/a$, $\bar{x} \equiv x/x_{\mathrm{sc}}$, and $\bar{\zeta} \equiv \zeta/F_c$ we can bring the equation of motion (8) into the dimensionless form

$$\partial_{\bar{t}}\bar{z} = -\partial_{\bar{x}}^4\bar{z} - (|\bar{z}| - 1) + \bar{\zeta} . \qquad (12)$$

For general types of potentials such as periodic potentials or power law potentials $V(z) \sim z^n$ with exponents $n \neq 2$, the equation of motion (8) is non-linear. Only for a parabolic potential with $n = 2$, the equation (8) is a linear partial differential equation, and an analytical solution can be easily found. For the above piecewise parabolic potential (3) we can therefore find analytical solutions of (8) in the domains $z > 0$ and $z < 0$ separately that will be matched by continuity conditions at $z = 0$.

In the Hamiltonian (2) we consider a semiflexible polymer with fixed *projected* length. This is a good approximation if fluctuations of the contour length are small. We can also consider a section of fixed projected length L of a longer polymer such that the contour length of this polymer section fluctuates by coupling to the polymer length reservoir provided by the rest of the polymer. The resulting equation of motion (8) in the ensemble with fixed projected length specifies the dynamics of the z-coordinate. If the polymer is inextensible, local conservation of contour length requires an additional longitudinal motion of the polymer segments in the x-direction [28–32]. We will discuss the effects from longitudinal motion of polymer segments in more detail in Section 9.5 below. We will show that kink motion does not require longitudinal motion of polymer segments and nucleation of a kink-antikink pair is mainly governed by the slow activated dynamics of the z-coordinate involved in barrier crossing, whereas contour length fluctuations happen on shorter time scales. Therefore the activated dynamics on a structured substrate is well described by the equation of motion (8) for the z-coordinate.

3 Static kink

In this section, we construct the *static kink*, which is a localized metastable excitation for $F = 0$ with the polymer ends in adjacent potential wells as shown in Figure 2. The static kink $z_k(x)$ is defined as the configuration that minimizes the energy (2), *i.e.*, is a time-independent solution of (8) in the absence of thermal noise ($\zeta = 0$). Thus it fulfills the inhomogeneous, piecewise linear differential equation

$$\begin{aligned}\kappa\partial_x^4 z + V_0(z + a) &= 0 , \qquad \text{for } z < 0 , \\ \kappa\partial_x^4 z + V_0(z - a) &= 0 , \qquad \text{for } z > 0 .\end{aligned} \qquad (13)$$

For $F = 0$, the potential is symmetric and $V(z) = V(-z)$ such that the kink configuration is antisymmetric with $z_k(x) = -z_k(-x)$ if we choose the x-coordinate such that the kink is centered at $x = 0$ (*i.e.* $z_k(0) = 0$). The static kink shape is given by boundary conditions that fix the end of the polymer in adjacent potential wells $z_k(\pm L/2) = \pm a$ with zero tangent $\partial_x z_k|_{\pm L/2} = 0$. We first

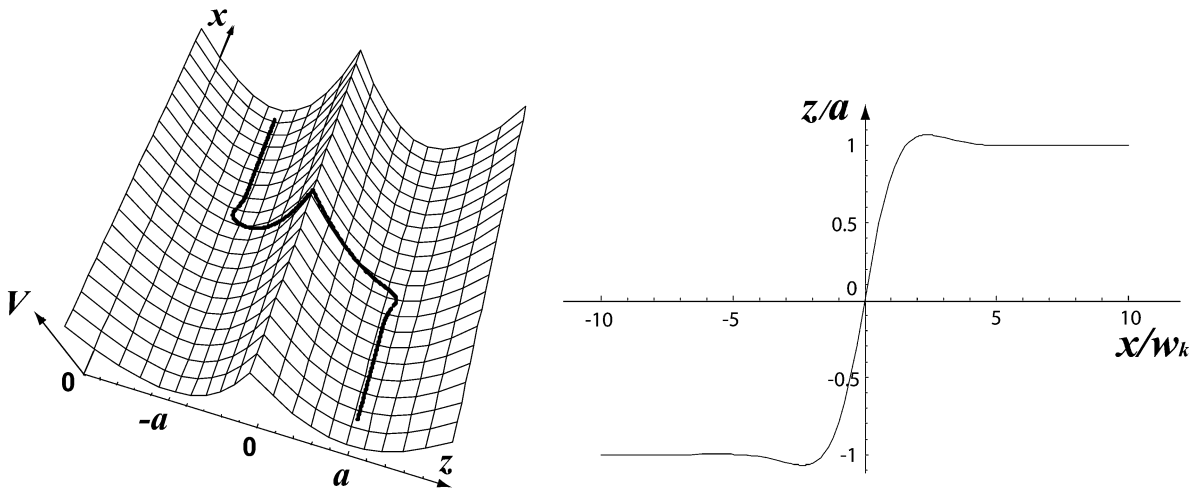

Fig. 2. Left: Conformation of a semiflexible polymer with a static kink ($F = 0$) in a double-well potential $V(z)$. Right: Polymer displacement z (in units of a) as a function of x (in units of w_k) for the same conformation with a static kink as shown on the left. The polymer length is $L = 20w_k$.

consider the two parts of the solution $z_{k+}(x)$ in the region $z_k > 0$ for $x > 0$ and $z_{k-}(x)$ in the region $z_k < 0$ for $x < 0$ separately. The homogeneous differential equation corresponding to (13) is the same for both parts and solved by linear combinations of the four functions $e^{\pm x/w_k} e^{\pm ix/w_k}$, where

$$w_k \equiv \sqrt{2} x_{\rm sc} = \sqrt{2} \left(\frac{\kappa}{V_0} \right)^{1/4} \tag{14}$$

is the kink width. The constant solutions $z_{k\pm}(x) = \pm a$ corresponding to a straight polymer in the potential minimum are particular solutions of the inhomogeneous equations (13) in the regions $z > 0$ and $z < 0$, respectively.

Therefore, the general solution of the equations (13) for both parts $z_{k+}(x)$ and $z_{k-}(x)$ of the static kink can be written in the following form:

$$\begin{aligned} z_{k\pm}(x) = {} & C_{1\pm} \cos(\bar{x}) \cosh(\bar{x}) + C_{2\pm} \sin(\bar{x}) \cosh(\bar{x}) \\ & + C_{3\pm} \cos(\bar{x}) \sinh(\bar{x}) + C_{4\pm} \sin(\bar{x}) \sinh(\bar{x}) \pm a \,, \end{aligned} \tag{15}$$

where $\bar{x} \equiv x/w_k$ and $C_{i\pm}$ $(i = 1, \ldots, 4)$ are eight linear expansion coefficients. In addition to the four boundary conditions at $x = \pm L/2$, we have to fulfill five matching conditions at $x = 0$ which connect the two parts of the kink for $x < 0$ and $x > 0$ as our potential is defined piecewise. From equation (13) it follows that the fourth derivative of the solution $z_k(x)$ has a finite jump at $x = 0$ and thus all lower derivatives and the solution itself have to be continuous across $x = 0$. This leads to five matching conditions $z_{k-}(0) = z_{k+}(0) = 0$, $\partial_x^m z_{k-}|_{x=0} = \partial_x^m z_{k+}|_{x=0}$ for $m = 1, 2, 3$. Two of the five matching condition turn out to be equivalent because the potential is symmetric and the kink-configuration is antisymmetric. The 8 linear expansion coefficients $C_{i\pm}$ $(i = 1, \ldots, 4)$ that are included in the solution Ansatz (15) are determined from the 8 independent boundary and matching conditions as a function of the system size L. As it is not instructive to display the details of the resulting formulae for the expansion coefficients $C_{i\pm}$, Figure 2 displays an example for a kink shape determined by this procedure. Figure 2 clearly shows that $z_k(x)$ is a non-monotonous function of x which is a fingerprint of the bending energy.

The kink energy is given by the Hamiltonian (2) as

$$\begin{aligned} E_k = {} & \int_{-L/2}^{0} {\rm d}x \left[\frac{\kappa}{2} \left(\partial_x^2 z_{k-} \right)^2 + \frac{1}{2} V_0 (z_{k-}(x) + a) \right] \\ & + \int_{0}^{L/2} {\rm d}x \left[\frac{\kappa}{2} \left(\partial_x^2 z_{k+} \right)^2 + \frac{1}{2} V_0 (z_{k+}(x) - a) \right] . \end{aligned} \tag{16}$$

The x-integration over the length L of the kink in (16) can be performed to obtain an explicit expression for the kink energy

$$E_k(L) = \frac{E_{\rm sc}}{\sqrt{2}} \frac{2 + \cos(L/w_k) + \cosh(L/w_k)}{\sinh(L/w_k) - \sin(L/w_k)} \,. \tag{17}$$

The kink energy $E_k(L)$ is minimal in the thermodynamic limit of infinite L, where we find

$$E_k = \frac{1}{\sqrt{2}} E_{\rm sc} = \frac{1}{\sqrt{2}} a^2 \kappa^{1/4} V_0^{3/4} \,. \tag{18}$$

We expect our results for the kink energy $E_k \sim E_{\rm sc}$ and kink width $w_k \sim x_{\rm sc}$ to hold for all potentials with a barrier height $\sim V_0 a^2$ and potential minima separation $\sim a$ independent of the particular potential form; only numerical prefactors will differ. The results (14) for the kink width and (18) for the kink energy depend only on the bending rigidity κ and the barrier height V_0, *i.e.*, the material properties of the semiflexible polymer and the substrate. These results also differ in their functional from analogous results for elastic strings or flexible polymers as they depend crucially on the bending rigidity. We also want to point out that measurements of the kink width w_k and the critical force density F_c or the kink energy E_k are sufficient to

determine the bending rigidity $\kappa = F_c w_k^4/4a = E_k w_k^3/2a^2$ and thus the persistence length $L_p = 2\kappa/T$ if the distance $2a$ between potential minima is known.

A semiflexible polymer will stay localized to the potential wells even if we set $V(z) = 0$ for $|z| > 2a$ as long as $V_0 > V_{0,c}$ with $V_{0,c}a^2 \simeq (T/L_p)(L_p/a)^{2/3}$ according to [19]. This condition is equivalent to $E_k \gtrsim T$ and thus a small density of thermally induced kink excitations. A small kink density in combination with the condition $L_p \gg a$ also ensures that the semiflexible polymer stays oriented along the x-axis such that the Hamiltonian (2) stays valid. The condition $E_k \gg T$ of a small kink density is equivalent to $L_p \gg w_k^3/a^2$ or $L_p \gg T^3/a^8V_0^3$. For sufficiently strong substrate potentials this gives a much wider range of applicability of the Hamiltonian (2) than in the absence of a potential, where the condition $L_p > L$ of weak bending has to be fulfilled for a semiflexible polymer to be oriented.

In the following we will focus on the regime $E_k \gg T$ which is also the regime where the dynamics of the semiflexible polymer is governed by thermal activation and the nucleation of kinks. In the opposite limit $E_k \ll T$, the semiflexible polymer shows essentially free fluctuations on the surface or even desorbs from the surface. In this regime the potential (3) can be treated perturbatively.

4 Stability of the kink-antikink pair

The static single kink in a system of size L is equivalent to one half of a symmetric *kink-antikink pair* configuration as shown in Figure 1 with kink-antikink separation $d = L$ in a system of size $2L$. The kink-antikink interaction energy $E_{\rm int}(d) = 2(E_k(d) - E_k(\infty))$ can thus be found by determining the single-kink energy in a finite system of length $L = d$. For $d/w_k \gg 1$ we read off from (17) an exponential decay

$$E_{\rm int}(d) \approx 2E_k[2 + \cos(d/w_k) + \sin(d/w_k)]e^{-d/w_k} \ , \quad (19)$$

where the oscillating prefactor is characteristic of semiflexible behaviour dominated by bending energy.

To test the stability of the kink-antikink configuration with distance $d = L$ against spontaneous recombination, we can numerically calculate the energy $E_k(L, z_f)$ of a "restricted" kink in a kink-antikink pair with boundary conditions $\partial_x z_k|_{+L_1/2} = 0$, $\partial_x z_k|_{-L_2/2} = 0$ $z_k(-L_2/2) = -a$ and another end of the kink (*i.e.*, the midpoint of the kink-antikink pair) fixed at $z_k(L_1/2) = z_f$. We introduce L_1 and L_2 with $L_1 + L_2 = 2L$ as the total length of the kink-antikink pair because the restricted kink is no longer antisymmetric. Still it is convenient to choose the midpoint of the kink at zero, $z_k(0) = 0$. As for the equilibrium configuration of the static kink, we have five matching conditions in $x = 0$. The energy of the kink-antikink configuration as a function of the midpoint of the kink-antikink pair z_f for different ratios L/w_k is shown in Figure 3. For $z_f = a$ we obtain again the single-kink energy and find that it is locally stable against z_f-variation for sufficiently large $L/w_k > 3.1$. The kink becomes unstable meaning that the equivalent kink-antikink pair spontaneously annihilates for small separations $L/w_k < 2.55$. In the regime $2.55 < L/w_k < 3.1$ the kink is locally stable for $z_f < a$, see Figure 3.

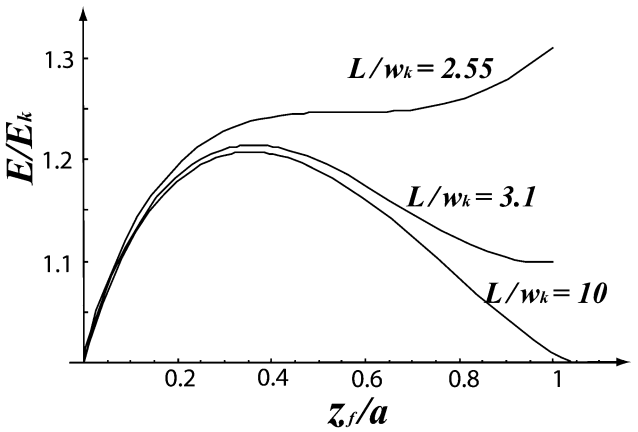

Fig. 3. Energy $E_k(L/w_k, z_f/a)$ (in units of $2E_k$) of a "restricted" kink as a function of the end point z_f (in units of a) and the kink-antikink distance L (in units of w_k) for a semiflexible polymer of total length $2L$. For distances $L/w_k > 3.1$ the kink is locally stable at $z_f/a = 1$, for $2.55 < L/w_k < 3.1$ the locally stable kink is obtained for $z_f/a < 1$, and for $L/w_k < 2.55$ it becomes unstable.

5 Moving kink

A driving force density F leads to an asymmetry in the potential and an effective force on kinks. Moving a kink by $-\Delta x$ increases the polymer length in the lower potential minimum by Δx and leads to an energy gain $-2aF\Delta x$ and thus a constant force

$$\mathcal{F}_k = -2aF \quad (20)$$

on a kink. As argued above, deviations from kink interactions are exponentially small for separations much larger than the kink width $d \gg w_k$. The force $\mathcal{F}_k$ leads to kink motion such that we also have to consider *moving kink* solutions. For constant kink velocity v the kink configuration assumes a form $z_k(x,t) = z_k(x - vt)$ that solves (8) for $\zeta = 0$. Transforming into the comoving frame of the kink by introducing the new coordinate $y \equiv x - vt$, the equation of motion (8) reduces to

$$\kappa\partial_y^4 z_k - v\gamma\partial_y z_k + V'(z_k) = 0, \quad (21)$$

which has to be solved with boundary conditions as for the static kink. However, in the asymmetric potential the kink is no longer antisymmetric such that the kink is centered at $y_0 \neq 0$, (*i.e.* $z_k(y_0) = 0$), where we also have to evaluate the matching conditions which are otherwise the same as for the static kink. The coordinate system of the static kink is inconvenient here, and calculations are simplified by translating the center of the kink to $y_0 = 0$ and introducing two different lengths L_1 and L_2 with $L_1 + L_2 = 2L$.

As for a static kink, we have four boundary conditions $\partial_y z_k|_{+L_1/2} = 0$, $\partial_y z_k|_{-L_2/2} = 0$, $z_k(-L_2/2) = z^-_{\min}$, $z_k(-L_1/2) = z^+_{\min}$. Analogously to (13), equation (21) is an inhomogeneous, piecewise linear differential equation due to the piecewise definition of the potential (3). We therefore consider the two parts of the moving kink solution $z_{k+}(y)$ in the region $z_k > 0$ for $y > 0$ and $z_{k-}(y)$ in the region $z_k < 0$ for $y < 0$ separately. Particular solutions of the inhomogeneous equation are the constant solutions $z_{k\pm}(y) = z^\pm_{\min}$ that correspond to straight polymers in the potential minima. For a moving kink both parts $z_{k\pm}(y) - z^\pm_{\min}$ solve the homogeneous differential equation corresponding to (21). Therefore, they are linear combinations of the four functions $e^{K_n y}$, where K_n $(n = 1, ...4)$ are the four roots of the equation

$$\kappa K_n^4 - v\gamma K_n + V_0 = 0 \; . \tag{22}$$

We find the four roots

$$K_n = \frac{1}{w_k}\left[\pm\sqrt{H(\bar v)} \pm \sqrt{-H(\bar v) \pm \frac{2^{3/2}\bar v}{3^{3/4}\sqrt{H(\bar v)}}}\right], \tag{23}$$

where the first and third sign have to be identical and $\bar v \equiv 3^{3/4} v/4v_{\rm sc}$ is a dimensionless velocity. The function

$$H(\bar v) \equiv \frac{(\bar v^2 + \sqrt{\bar v^4 - 1})^{2/3} + 1}{\sqrt{3}(\bar v^2 + \sqrt{\bar v^4 - 1})^{1/3}} \tag{24}$$

has the following properties: $H(\bar v)$ is real and positive for any velocity $\bar v > 0$ and has a minimum in $\bar v = 0$, where $H(\bar v) \geq H(0) = 1$. $H(\bar v)$ is monotonically increasing with the asymptotics $H(\bar v) \propto 1 + \bar v^2/3\sqrt{3} + O(\bar v^4)$ for $\bar v < 1$ and $H(\bar v) \propto \bar v^{2/3}$ for $\bar v \gg 1$. These properties of the function $H(\bar v)$ allow to simplify the calculation because in the limit of large system sizes $L \gg w_k$ one can neglect in the moving kink solution all exponentially decreasing terms $\sim \exp(-\sqrt{H(\bar v)}L/2w_k)$.

The width of the moving kink is determined by the real parts of the four roots K_n as given by (23). As opposed to the static kink, the moving kink solution with $v > 0$ is not antisymmetric such that the real parts of the four roots need not have the same absolute value. Then, the moving kink can have two different widths $w_{k,+}(v)$ and $w_{k,-}(v)$ in the directions $y > 0$ and $y < 0$, respectively, which are determined by the roots with negative and positive real parts, respectively,

$$w_{k,\pm} = \frac{1}{\min_{{\rm Re}[K_n]\lessgtr 0}\{|{\rm Re}[K_n(v)]|\}} \; . \tag{25}$$

For small velocities $\bar v < 1$, the real parts of all four roots have the same absolute value $|{\rm Re}[K_n(v)]| = \sqrt{H(\bar v)}/w_k$ such that

$$w_{k,+}(v) = w_{k,-}(v) = \frac{w_k}{\sqrt{H(\bar v)}} \; . \tag{26}$$

Thus, the kink width decreases with velocity, and we find $w_k(v) \approx w_k(1 - \bar v^2/6\sqrt{3} + O(\bar v^4))$ for small velocities $\bar v \ll 1$. For large velocities $\bar v > 1$, on the other hand, the real parts differ and we find

$$\begin{aligned} w_{k,+}(v) &= \frac{w_k}{\sqrt{H(\bar v)}} \, , \\ w_{k,-}(v) &= \frac{w_k}{\sqrt{H(\bar v)} - \sqrt{-H(\bar v) + \frac{2^{3/2}\bar v}{3^{3/4}\sqrt{H(\bar v)}}}} \, , \end{aligned} \tag{27}$$

which shows that $w_{k,-} > w_{k,+}$ as can also be seen in Figure 4. For large velocities $\bar v \gg 1$, $|{\rm Re}[K_n]| \propto \bar v^{1/3}$ for all four roots, and both kink widths vanish as $w_{k,\pm}(v) \propto w_k \bar v^{-1/3}$.

The general solution of the equations (21) for both parts $z_{k+}(y)$ and $z_{k-}(y)$ of the moving kink can be written in the following form:

$$z_{k\pm}(y) = \sum_{n=1}^{4} C_{n\pm} e^{K_n y} + z^\pm_{\min} \tag{28}$$

with eight linear expansion coefficients $C_{i\pm}$ $(i = 1, \ldots, 4)$ that have to be determined by the four boundary conditions and matching conditions at $y = 0$. Analogously to the static kink, we have also for the moving kink the five matching conditions $z_{k-}(0) = z_{k+}(0) = 0$, $\partial_x^m z_{k-}|_{y=0} = \partial_x^m z_{k+}|_{y=0}$ for $m = 1, 2, 3$. Together with the four boundary conditions and $2L = L_1 + L_2$ we have 10 conditions to determine the 10 parameters $C_{i\pm}$ $(i = 1, \ldots, 4)$, L_1, and L_2 as a function of the system size L and the remaining parameters of the model. The shape of a moving kink that we obtain using this procedure is shown in Figure 4.

However, in the thermodynamic limit of infinite L_1 and L_2, we are left with 8 parameters $C_{i\pm}$ $(i = 1, \ldots, 4)$ to be determined by 9 boundary and matching conditions. Therefore, in the thermodynamic limit, a moving kink solution fulfilling all boundary and matching conditions can only be found for certain values of v for given F. These values are determined by the remaining matching condition after we determined all eight expansion coefficients $C_{i\pm}$ $(i = 1, \ldots, 4)$. Following this procedure we find after a rather lengthy calculation the force-velocity relation

$$F(\bar v) = -F_c \bar v \frac{3^{1/4} 2^{-1/2} H^{3/2}(\bar v)}{H^3(\bar v) + 3^{-3/2}\bar v^2} \tag{29}$$

in the thermodynamic limit. For small forces we find a linear response $F = -3^{1/4}2^{-1/2}F_c\bar v$, close to the critical force F_c the velocity diverges as $-\bar v \sim (1 - F/F_c)^{-3/2}$, see Figure 5.

The result (29) can also be used to obtain the friction constant η_k of a moving kink as force-equilibrium requires $\mathcal{F}_f + \mathcal{F}_k = 0$ with the friction force $\mathcal{F}_f = -v\eta_k$ and the driving force $\mathcal{F}_k = -2aF$ which gives the relation

$$\eta_k = 2a|F(v)|/v \; . \tag{30}$$

In the limit of small velocities v, the above relation (29) is linear and we find

$$\eta_k(v) \approx \frac{3}{2^{3/2}} \frac{aF_c}{v_{\rm sc}} = \frac{3}{2}\frac{\gamma a^2}{w_k} \; . \tag{31}$$

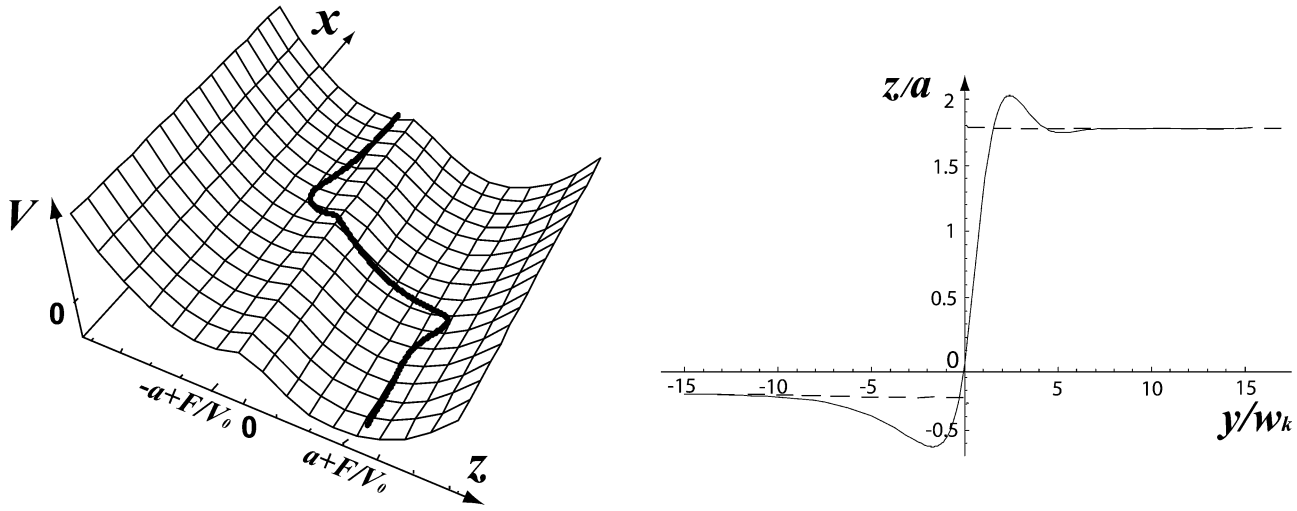

Fig. 4. Left: Conformation of a semiflexible polymer with a moving kink in a double-well potential $V(z)$ in the presence of a driving force $F > 0$. Right: Polymer displacement z (in units of a) as a function of $y = x - vt$ (in units of w_k) for the same conformation with a moving kink as shown on the left. The driving force is $F = 0.775F_c$, leading to a kink velocity $v = 2^{-1/2}v_{\rm sc}$ or $\bar{v} = 3^{3/4}2^{-1/2} \approx 1.6$. The total length of the polymer is $2L = L_1 + L_2 = 60w_k$ with $L_1 = L_2 = 30w_k$. Dashed lines show the potential minima at $z^{\pm}_{\rm min}/a = \pm 1 + F/F_c$.

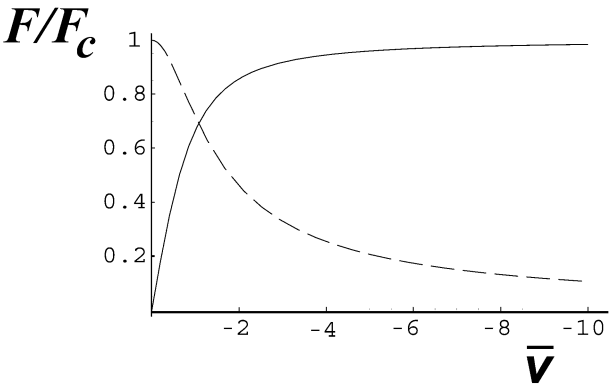

Fig. 5. Force density F (in units of F_c, solid line) and friction constant η_k (in units of $3F_c a/2^{3/2}v_{\rm sc} = 3a^2\gamma/w_k$, dashed line) as a function of velocity $\bar{v} = 3^{3/4}v/4v_{\rm sc}$ for a moving kink.

The friction constant η_k is also related to the energy dissipation rate $\mathrm{d}E/\mathrm{d}t$ due to kink motion which is defined as the product of friction force, $-v\eta_k$, and velocity, $\mathrm{d}E/\mathrm{d}t = -v^2\eta_k$. On the other hand, $\mathrm{d}E/\mathrm{d}t$ can be calculated directly using the equations of motion (8) and (21) in the limit of large L

$$\frac{\mathrm{d}E}{\mathrm{d}t} = \int_{-\infty}^{\infty} \mathrm{d}x \frac{\delta \mathcal{H}}{\delta z_k}(\partial_t z_k) = -\gamma v^2 \int_{-\infty}^{\infty} \mathrm{d}x \left(\partial_x z_k\right)^2 , \quad (32)$$

and we read off a kink friction constant

$$\eta_k = \gamma \int_{-\infty}^{\infty} \mathrm{d}x \left(\partial_x z_k\right)^2 . \quad (33)$$

In the limit of small driving forces F and velocities v we can use the static kink configuration in (33), perform the x-integration and find again $\eta_k(v) \approx 3\gamma a^2/2w_k$ for small v in agreement with the result (31).

Apart from a numerical prefactor, the force-velocity relationship in the linear response regime can also be obtained by a simple scaling argument. For small velocities the kink solution is similar to a static kink with length scales scaling as $z \sim a$ and $x \sim w_k$. We argue that the driving force F and the left-hand side in (8) scale in the same way, $F \sim \gamma z/t$, which sets a time scale $t \sim \gamma a/F$ for kink motion. The resulting kink velocity is given by the ratio $v \sim w_k/t \sim Fw_k/\gamma a$, which is identical to the linear response regime of (29).

6 Effect of noise on the kink motion

In the previous section we determined the kink velocity in the presence of the driving force F but we effectively considered the case of zero temperature and neglected all effects from the thermal random force, which leads to a diffusive component in the kink motion. For a more detailed analysis of the effect of noise on the kink motion we consider noise-induced perturbations of shape and velocity of a kink moving with constant velocity v. For a time-dependent kink center at $x_k(t)$ the comoving frame coordinate is given by $\bar{y} \equiv x - x_k(t)$. Adding shape perturbations to the corresponding kink solution $z_k(\bar{y})$ of equation (21), we arrive at the decomposition

$$z(x,t) = z_k(x - x_k(t)) + \sum_{p=1}^{\infty} X_p(t)\phi_p(x - x_k(t), t) . \quad (34)$$

ϕ_p are normal modes of the chain in the presence of the kink which we will determine below and $X_p(t)$ are expansion coefficients; the zero mode of kink translation is explicitly taken into account by positioning the kink center

at $x_k(t)$. Substituting (34) into the equation of motion (8), expanding about the kink, and retaining first-order terms in $X_p(t)$, we obtain

$$\gamma(v-\dot{x}_k(t))\partial_{\bar{y}}z(\bar{y})+\sum_{p=1}^{\infty}X_p(t)\hat{\mathcal{L}}\phi_p(\bar{y},t)$$
$$+\gamma\sum_{p=1}^{\infty}\dot{X}_p(t)\phi_p(\bar{y},t)=\zeta(x,t), \tag{35}$$

where the operator $\hat{\mathcal{L}}$ is defined as

$$\hat{\mathcal{L}}\equiv\gamma\partial_t+\kappa\partial_{\bar{y}}^4-\gamma\dot{x}_k(t)\partial_{\bar{y}}+V''(z(\bar{y}))\ . \tag{36}$$

If the normal modes fulfill the condition

$$\left(\gamma\partial_t+\kappa\partial_{\bar{y}}^4-\gamma v\partial_{\bar{y}}+V''(z(\bar{y}))\right)\phi_p=0\,, \tag{37}$$

equation (35) becomes

$$\gamma(v-\dot{x}_k(t))\left(\partial_{\bar{y}}z(\bar{y})+\sum_{p=1}^{\infty}X_p(t)\partial_{\bar{y}}\phi_p(\bar{y},t)\right)$$
$$+\gamma\sum_{p=1}^{\infty}\dot{X}_p(t)\phi_p(\bar{y},t)=\zeta(x,t)\,. \tag{38}$$

Using an Ansatz $\phi_p(\bar{y},t)=f_p(\bar{y})e^{-\omega_p t}$ in (37) the normal modes are determined by the eigenvalue equation

$$\kappa\partial_{\bar{y}}^4f_p-\gamma v\partial_{\bar{y}}f_p+V''(z_k(\bar{y}))f_p=\omega_p\gamma f_p\,, \tag{39}$$

where $V''(z)=V_0(1-2a\delta(z))$. Equation (39) has a set of eigenvalues ω_p with orthonormal eigenfunctions $f_p(\bar{y})$ with respect to the scalar product

$$\langle f|g\rangle\equiv r^{-1}\int_{-L/2}^{L/2}\mathrm{d}\bar{y}f(\bar{y})g(\bar{y})\ \text{ with }\ r\equiv a^2w_k\ , \tag{40}$$

where the division by the dimensionful constant r makes the scalar product dimensionless [33]. For a very long polymer $L/2\gg x_k(t)$ the influence of the ends on the dynamics of barrier crossing can be neglected. Therefore, we can neglect the shift of boundaries in the comoving frame and use $\bar{y}\approx\pm L/2$ for the coordinates of the polymer ends in the comoving frame in (40). Then, the eigenvalue problem has to be solved with boundary conditions $f_p(-L/2)=f_p(L/2)=0$, $f_p'(-L/2)=f_p'(L/2)=0$ and matching conditions $f_{p+}^{(m)}(0)=f_{p-}^{(m)}(0)$ for $m=0,1,2$. Integrating the equation (39) between $\bar{y}=-\varepsilon$ and $\bar{y}=+\varepsilon$, then letting ε approach zero, one finds that the third derivative of the eigenfunction $f_p(\bar{y})$ has a discontinuity at $\bar{y}=0$. This gives an additional matching condition $f_{p+}^{(3)}(0)-f_{p-}^{(3)}(0)=2aV_0f_p(0)/\kappa|\partial_{\bar{y}}z_k|$. The translation mode

$$f_0=\partial_{\bar{y}}z_k(\bar{y})/C \tag{41}$$

of the kink is a zero mode corresponding to the solution with eigenvalue $\omega_0=0$. C is a normalization constant determined by

$$C^2=\langle\partial_{\bar{y}}z_k|\partial_{\bar{y}}z_k\rangle=r^{-1}\int_{-L/2}^{L/2}\mathrm{d}\bar{y}\,(\partial_{\bar{y}}z_k)^2\ . \tag{42}$$

Multiplying equation (38) with the translation mode $f_0(\bar{y})$ and integrating yields an equation of motion for the kink

$$\dot{x}_k(t)=v+\zeta_k(t)\left[1+C^{-1}\sum_{p=1}^{\infty}X_p(t)e^{-\omega_p t}\langle f_0|\partial_{\bar{y}}f_p\rangle\right]^{-1}. \tag{43}$$

Because of the orthogonality $\langle f_0|f_p\rangle=0$ contributions from the first sum in (38) vanish. The variable $\zeta_k(t)$ is an effective Gaussian thermal noise for the kink as given by

$$\zeta_k(t)=-(C\gamma r)^{-1}\int_{-L/2}^{L/2}\mathrm{d}\bar{y}f_0(\bar{y})\zeta(\bar{y}+x_k(t),t) \tag{44}$$

with correlations $\langle\zeta_k(t)\zeta_k(t')\rangle=\delta(t-t')(2T/C^2\gamma r)$ (where we used $\langle f_0|f_0\rangle=1$). Multiplying equation (38) with the modes $f_p(\bar{y})$ and integrating yields the equation of motion for the amplitudes $X_p(t)$

$$\dot{X}_p(t)=\zeta_p(t), \tag{45}$$

where $\zeta_p(t)=\gamma^{-1}\int\mathrm{d}\bar{y}f_p(\bar{y})\zeta(\bar{y}+x_k(t),t)$. A solution of equation (45) is $X_p(t)=\text{const}+\int_0^t\mathrm{d}t'\zeta_p(t')$.

The sum in the bracketed term in (43) represents terms from kink-phonon scattering which decay exponentially for times $t>1/\omega_p$. Neglecting the kink-phonon scattering leads to an overdamped Langevin equation for the kink position

$$\dot{x}_k(t)=v+\zeta_k(t) \tag{46}$$

describing Brownian motion with drift. From the noise correlations we can read off the corresponding diffusion constant of the kink as

$$D_k=\frac{T}{C^2\gamma r}\,. \tag{47}$$

Note that the corresponding kink friction constant

$$\eta_k=\frac{T}{D_k}=\frac{C^2}{\gamma r}=\gamma\int_{-L/2}^{L/2}\mathrm{d}\bar{y}\,(\partial_{\bar{y}}z_k)^2 \tag{48}$$

is identical to our above result (33) obtained from complementary energetic considerations in the limit of large L.

7 Kink motion and relaxation

If kink-phonon scattering is neglected, a single kink performs Brownian motion with drift. The kink diffusion constant D_k is given by (47), the driving force F leads to a force $\mathcal{F}_k=-2aF$ on the kink, see (20), and to a directed motion with mean velocity $v(F)$ as calculated in (29). A semiflexible polymer in a configuration with a single kink crosses the potential barrier by moving the kink over the entire length L of the polymer. Thus, the average crossing time is $t_{\mathrm{cr}}\sim L/v=L\eta_k/2aF$ (see Eq. (30)) for the case of directed diffusion under the influence of a driving force F giving rise to $v>0$. In the absence of a driving force $F=0$, we have $v=0$ and the kink performs an unbiased

random walk with $\langle (x_k(t) - x_k(0))^2 \rangle \approx 2D_k t$ from which we estimate the average crossing time as $t_{\rm cr} \sim L^2/2D_k = L^2\eta_k/2T$, which becomes $t_{\rm cr} \sim L^2\gamma a^2/Tw_k$ using (31) in the regime of small velocities. To be more precise the average crossing time can be identified with the mean first passage time of the diffusing kink for a distance L under the external force $\mathcal{F}_k$, which is given by [34]

$$t_{\rm cr} \approx \frac{L^2}{D_k}\left(\frac{T}{|\mathcal{F}_k|L}\right)^2\left(e^{-|\mathcal{F}_k|L/T} - 1 + \frac{|\mathcal{F}_k|L}{T}\right). \quad (49)$$

From (49) we indeed recover our above estimates for random, diffusion-dominated motion in the limit of small forces $F \ll T/La$ and directed, drift-dominated motion in the limit of large forces $F \gg T/La$.

Now we consider the relaxation of a kink-antikink pair by annihilation in the absence of a force, $F = 0$. Then, the motion of the kinks is purely diffusive. For $F = 0$ the potential is symmetric and according to our discussion in Section 4 the kink-antikink pair becomes unstable if its separation L is sufficiently small $L < 2.55w_k$, see Figure 3. Therefore, in order to annihilate, the kink-antikink pair has to diffuse over a distance $L - 2.55w_k$ which is of the order of L if $L \gg w_k$. Then it can spontaneously annihilate, and the polymer reaches its final kinkless state of a straight-line configuration in one potential well. Therefore, the relaxation process takes a time $t_{\rm rel} \sim L^2\eta_k/T \sim L^2\gamma/Tw_k$ which is of the same order as the diffusive crossing time of a single kink on a polymer of total length L.

8 Kink nucleation rate and kink density

Thermally activated barrier crossing proceeds by the production and subsequent motion of kinks. So far, we have considered the motion of single kinks after they have been created, *e.g.*, by nucleation. The kink production is characterized by the nucleation rate j which is defined as the total number of kink-antikink pairs nucleated per time and polymer length. Before we consider the kink nucleation in detail and calculate j in the following sections, we want to describe the stationary state with the dynamical equilibrium between kink production and kink annihilation. The dynamical equilibrium involves many interacting kinks and depends on the kink density ρ. We consider an ensemble of ρL kinks and ρL antikinks with kink density $\rho \ll 1/w_k$ as in Figure 6, *i.e.*, the mean distance that a kink travels before annihilation is $d = 1/\rho$.

For sufficiently large F, the kink motion is directed, the diffusive component of the kink motion can be neglected, and kinks move with mean velocity $v = aF/\eta_k$ (see Eq. (30)). The relative velocity of a kink moving towards an antikink is $2v$ and the average lifetime of a kink in this regime is thus $\tau_F = d/2v = 1/2\rho v$, see Figure 6. The dynamic equilibrium between kink annihilation and production is reached for $j = \rho/\tau_F = 2\rho^2 v$, as previously derived for kink excitations of elastic strings [10].

For small F, the kink motion is diffusion-dominated with a diffusion constant D_k given by (47) for a single kink. The relative motion of a kink and antikink is also diffusive with an effective diffusion constant $2D_k$ and their mean-square separation obeys $\langle \Delta x_k^2 \rangle = 4D_k t$. Then, the average lifetime in this regime is $\tau_D = d^2/4D_k = 1/4\rho^2 D_k$. The dynamic equilibrium for kink annihilation and production is reached for $j = \rho/\tau_D = 4\rho^3 D_k$ [35].

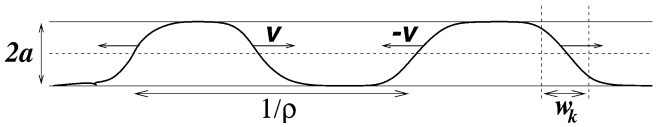

Fig. 6. An ensemble of well-separated kinks and antikinks ($\rho < 1/w_k$) which move with velocity v and $-v$, respectively.

The crossover between both regimes takes place if $\tau_F = \tau_D$ which defines a characteristic force

$$F_\rho \equiv \frac{T\rho}{a}. \quad (50)$$

Thus, the kink nucleation rate j and the kink density ρ satisfy the relations and we have

$$j = 2v\rho^2, \qquad \text{for } F \gg F_\rho, \quad (51)$$

and

$$j = 4D_k\rho^3, \qquad \text{for } F \ll F_\rho. \quad (52)$$

9 Kink nucleation

In this section we want to study the nucleation of kinks and determine the nucleation rate j by Kramers theory for large driving forces and by quasi-equilibrium considerations for small forces.

9.1 Critical nucleus

As for flexible strings [6,7,10] the dynamics of the nucleation is governed by the critical nucleus representing the saddle point configuration in the multi-dimensional energy landscape in the presence of a force $F > 0$. An example for a critical nucleus configuration of a semiflexible polymer is shown in Figure 7. In the limit $F = 0$ the critical nucleus reduces to a static kink-antikink pair. The critical nucleus $z_n(x)$ fulfills the saddle point equation $\delta\mathcal{H}/\delta z = 0$ for the energy (2)

$$\begin{aligned} &\kappa\partial_x^4 z + V_0(z+a) - F = 0, \qquad \text{for } z < 0, \\ &\kappa\partial_x^4 z + V_0(z-a) - F = 0, \qquad \text{for } z > 0 \end{aligned} \quad (53)$$

with the full asymmetric potential (3) for $F > 0$. We introduce two parts of the solution, $z_{n+}(x)$ in the region $z_n > 0$ and $z_{n-}(x)$ in the region $z_n < 0$. In the limit $F = 0$ the saddle point equation (53) for the critical nucleus reduces to the corresponding equation (13) for static kinks. In particular, the homogeneous differential equation corresponding to (53) is identical to that for static kinks. Therefore, the critical nucleus configuration can be constructed as a sum of a linear combination of the four

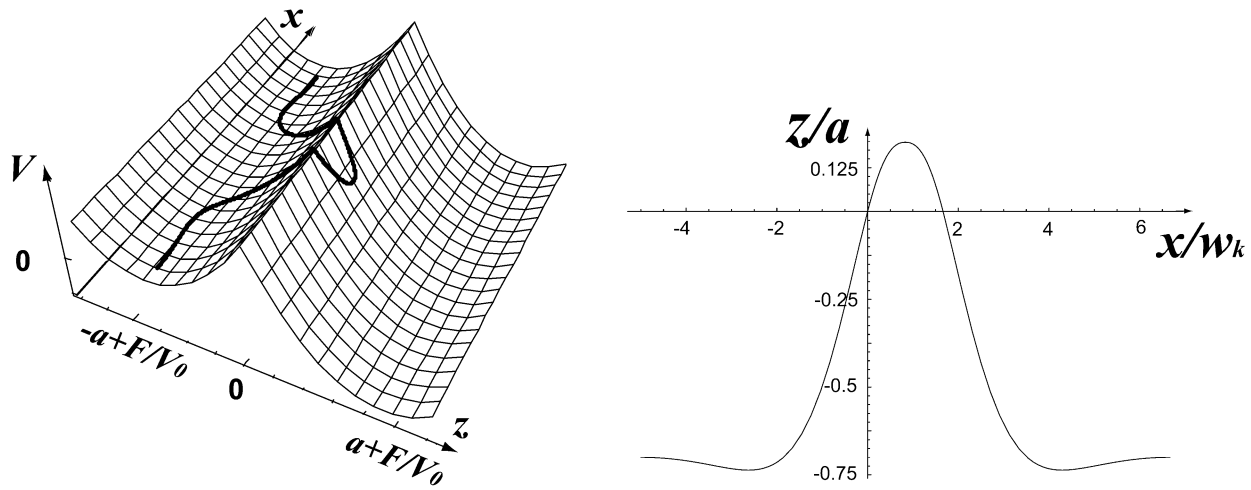

Fig. 7. Left: Critical nucleus conformation of a semiflexible polymer in a double-well potential $V(z)$ in the presence of a driving force $F > 0$. Right: Polymer displacement z (in units of a) as a function of x (in units of w_k) for the same critical nucleus conformation shown on the left. The driving force is $F = 0.25F_c$. The total length of the polymer is $L + L'$. For $L = 10w_k$, we find $L' \approx 1.66w_k$ for the distance between the points where the potential barrier is crossed.

functions $e^{\pm x/w_k}e^{\pm ix/w_k}$ and a particular solution of the non-homogeneous equation (53). This gives

$$z_{n\pm}(x) = C_{1\pm}\cos(\bar{x})\cosh(\bar{x}) + C_{2\pm}\sin(\bar{x})\cosh(\bar{x}) + C_{3\pm}\cos(\bar{x})\sinh(\bar{x}) + C_{4\pm}\sin(\bar{x})\sinh(\bar{x}) + z^{\pm}_{\min}, \tag{54}$$

where $\bar{x} = x/w_k$ and $C_{i\pm}(i = 1, \ldots, 4)$ are eight linear expansion coefficients. In the following we exploit the mirror-symmetry of the critical nucleus around its midpoint and consider a "half-nucleus" which is analogous to a single static kink for $F = 0$. We choose the origin $x = 0$ such that $z_n(0) = 0$, and the half-nucleus extends from one end point at $x = -L/2$ to the midpoint the position of which we define as $x = L'/2$. The total length $L + L'$ of the critical nucleus is thus determined by L'. Due to the asymmetry of the potential the critical nucleus is shortened as compared to the static kink such that $L' < L$. For the critical nucleus we have the three boundary conditions $z_n(-L/2) = z^-_{\min}$ and $\partial_x z_n|_{-L/2} = \partial_x z_n|_{L'/2} = 0$, but with $z_n(L'/2) < z^+_{\min}$ at the midpoint. Additionally, we have the fourth boundary condition $\partial^3_x z_n|_{L'2} = 0$ because of the mirror symmetry of the critical nucleus configuration. As for the static kink we also have five matching conditions $z_{n-}(0) = z_{n+}(0) = 0$, $\partial^m_x z_{n-}|_{x=0} = \partial^m_x z_{n+}|_{x=0}$ for $m = 1, 2, 3$. In summary we have 9 conditions to determine the 9 parameters $C_{i\pm}(i = 1, \ldots, 4)$ and L' as a function of the length L and the remaining model parameters, in particular the the reduced force F/F_c. Using these conditions one can find that L' is given by

$$\cos(L'/w_k)e^{-L'/w_k} = F/F_c \tag{55}$$

in the limit $L \gg w_k$. As F approaches F_c, L' vanishes as $L' = w_k(1 - F/F_c)$. For small forces, on the other hand, the critical nucleus approaches a kink-antikink pair configuration with $L' \approx L$. Due to the oscillating left-hand side in (55) we find jumps in the length L' of the stable nucleus as a function of the force F, which are a signature of the semiflexible behaviour dominated by bending energy. For stable solutions of (55), we find $L'/w_k \approx -\ln(2F/F_c)$. The solution of equation (53) for the above boundary and matching conditions gives the shape of the nucleus that is shown in Figure 7.

The excess energy of the critical nucleus is given by

$$\Delta E_n = \int_{-L/2}^{L'/2} \mathrm{d}x \left[\frac{\kappa}{2}\left(\partial_x^2 z_n\right)^2 + V(z_n) - V(z^-_{\min})\right] . \tag{56}$$

It is not possible to find a closed analytical expression for the energy of the critical nucleus satisfying all boundary and matching conditions. However, it turns out that it is possible to calculate the energy (56) in the limit $L \gg w_k$ for the class of nucleus-like configurations that fulfill all boundary and matching conditions except $\partial^3_x z_n|_{L'2} = 0$. This class of configurations contains the critical nucleus as special case. With only 8 conditions we leave the length L' of the nucleus-like configuration undetermined, and after a lengthy calculation we obtain the resulting energy (56) of this configuration as a function of L' as

$$\Delta E_n(L') = 2E_k\left(1 - 2\frac{FL'}{F_c w_k} + 2e^{-L'/w_k}\sin^2(L'/2w_k) + \frac{F}{F_c}\frac{e^{L'/w_k}F/F_c - 2\cos(L'/w_k)}{1 + \sin(L'/w_k)}\right) . \tag{57}$$

Figure 8 shows the energy $\Delta E_n(L')$ as a function of L' for a given force F. From (57) it can be shown that the local maximum of the function $\Delta E_n(L')$ fulfills also the relation (55) and corresponds to the actual critical nucleus configuration that satisfies all 9 boundary and matching conditions. This demonstrates that the critical nucleus is a metastable configuration. Interestingly, the energy (57) also has a local minimum in which the relation

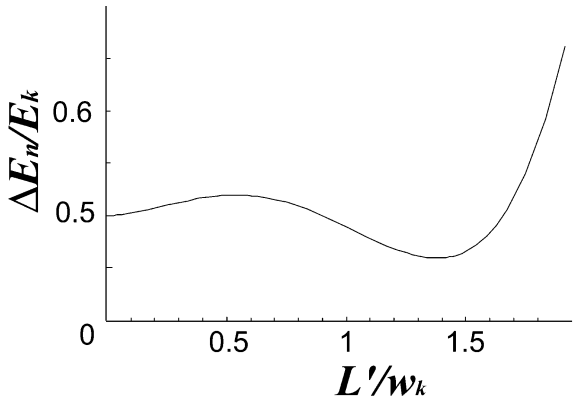

Fig. 8. The energy ΔE_n (in units of E_k) according to (57) as a function of L' (in units of w_k) for $F/F_c = 0.5$.

$(1 + \sin(L'/w_k))e^{-L'/w_k} = F/F_c$ holds, that turns out to be equivalent to the condition $\partial_x^2 z_n|_{L'2} = 0$. Although such a configuration lowers the energy, it has a discontinuity in $\partial_x^3 z_n(x)$ at the midpoint $x = L'2$. The existence of such a nucleus-like configuration with lower energy hints at a symmetric, unstable fluctuation mode of the critical nucleus that will be discussed in detail below.

Close to the critical force L' approaches zero according to (55), and the energy of the critical nucleus vanishes as

$$\Delta E_n \approx 2E_k \left(1 - \frac{F}{F_c}\right)^2 . \tag{58}$$

For small forces, the nucleus approaches a kink-antikink pair configuration with $L' \approx L$. For small forces we find $L'/w_k \approx -\ln(2F/F_c)$ from (55) and for the energy (57) of the critical nucleus

$$\Delta E_n \approx 2E_k \left(1 + 2\frac{F}{F_c} \ln\left(\frac{\sqrt{2}F}{F_c}\right)\right) . \tag{59}$$

This result is equivalent to an approximate description of the nucleus kink-antikink pair with distance L' with an energy $2E_k - 2aFL' + E_{\rm int}(L')$. The first term is the energy of the isolated kink-antikink pair, the second term the energy gain due to the force (20) pulling kink and antikink apart and the last term the interaction energy (19). Optimizing this energy with respect to L' gives the result (59) apart from corrections due to the shape changes [6,7,35].

In contrast to the kink width (14) and the kink energy (18) which depend only on the barrier height $\sim V_0 a^2$ and potential minima separation $\sim a$ (apart from numerical prefactors) the properties of the critical nucleus close to the critical force depend crucially on the detailed shape of the potential in the vicinity of the barrier. In general, we expect ΔE_n to vanish upon approaching the critical force F_c and to reduce to the kink energy E_k for small forces $F \ll F_c$ suggesting the scaling behaviour

$$\Delta E_n \sim E_k \left(1 - \frac{F}{F_c}\right)^\alpha \tag{60}$$

with an exponent α that depends on the shape of the potential barrier. Note that our above result (58) follows such a scaling law with an exponent $\alpha = 2$. The exponent α can be determined by employing a scaling argument for the critical nucleus, where we consider a general potential shape with a barrier height scaling as $V_F \sim V_0 a^2 (1 - F/F_c)^\epsilon$ and the distance between metastable minimum and barrier scaling as $z_F \sim a(1 - F/F_c)^\mu$ upon approaching the critical force F_c where both quantities vanish by definition. Note that the two exponents ϵ and μ are determined solely by the shape of the potential. The critical nucleus will then extend over a length L_n that is determined by the competition between the bending energy $\sim \kappa z_F^2/L^3$ and the potential energy $\sim LV_F$ which gives $L_n \sim w_k(1 - F/F_c)^{(2\mu-\epsilon)/4}$, where $w_k \sim (\kappa/V_0)^{1/4}$ is the kink width. The resulting energy ΔE_n of the critical nucleus scales as in (60) with an exponent $\alpha = (2\mu + 3\epsilon)/4$ and the kink energy $E_k \sim a^2 \kappa^{1/4} V_0^{3/4}$.

This general behaviour can be checked for our piecewise parabolic potential (3) for which we find a barrier height $V_F = V(0) - V(z_{\rm min}) = (V_0 a^2/2)(1 - F/F_c)^2$, *i.e.*, an exponent $\epsilon = 2$, and a critical displacement $z_F = |z_{\rm min}| = a(1 - F/F_c)$, *i.e.*, $\mu = 1$. This gives $\alpha = 2$ in accordance with the exact result (58) (note that $L_n \sim L' + w_k$ in this case). For a periodic potential $V_0 a^2(1 - \cos(2\pi z/a)) - Fz$, on the other hand, one finds $\epsilon = 3/2$ and $\mu = 1/2$ which leads to a different exponent $\alpha = 11/8$ although the static kink energies $E_k \sim a^2 \kappa^{1/4} V_0^{3/4}$ and the kink width $w_k \sim (\kappa/V_0)^{1/4}$ scale in the same way (although with different numerical prefactors) for both potential shapes. This demonstrates that properties of the critical nucleus are much less universal and much more dependent on the detailed shape of the potential close to the critical force F_c. At small forces the critical nucleus approaches a static kink configuration with a kink energy E_k and kink width w_k that are independent of the detailed shape of the potential.

9.2 Fluctuation eigenmodes

The energy of the critical nucleus (58) is the activation energy that, according to Kramers theory, enters the Arrhenius factor of the nucleation rate

$$j \sim \exp\left(-\frac{\Delta E_n}{T}\right), \tag{61}$$

which is the total number of kink-antikink pairs nucleated per time (per length). A systematic calculation of j requires to find the corresponding attempt frequencies and thus to add small perturbations $\delta z_n(x)$ and $\delta z_s(x)$ to the critical nucleus configuration $z_n(x)$ representing the saddle point and the straight configuration $z_s(x) = z_{\rm min}^-$ representing the initial energy minimum. We will investigate the stability of these solutions against small oscillations by analyzing the eigenmode spectrum of these fluctuations.

Expansion of the energy in the neighborhood of a stationary configuration to second oder of the perturbation

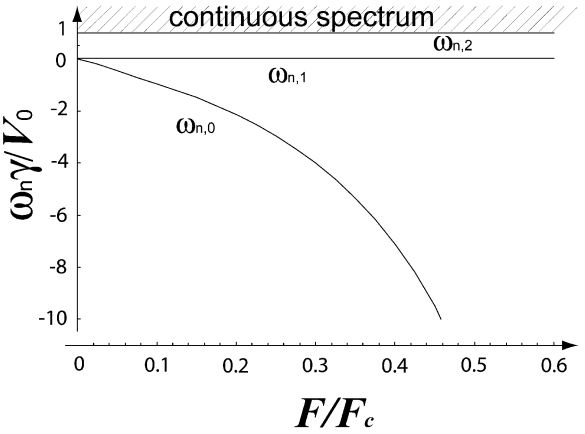

Fig. 9. Eigenvalues of the critical nucleus $\omega_{n,p}\gamma/V_0$ as functions of the force F/F_c in the thermodynamic limit of infinite L.

$\delta z_q(x)$ yields

$$\mathcal{H}\{z_q(x)+\delta z_q(x)\} \approx \mathcal{H}\{z_q(x)\} + \frac{1}{2}\int \mathrm{d}x \delta z_q(x)\left[\kappa\partial_x^4 + V''(z_q)\right]\delta z_q(x), \tag{62}$$

where $V''(z) = V_0(1-2a\delta(z))$ and the subscript q equals n or s corresponding to the critical nucleus or the straight configuration, respectively. We expand the perturbations $\delta z_q(x)$ in terms of normal modes $\delta z_q(x) = \sum_p X_p f_p(x)$ that fulfill an eigenvalue equation of the form (39) for $v = 0$,

$$\kappa\partial_x^4 f_p + V''(z_q(x))f_p = \omega_p \gamma f_p \tag{63}$$

with $V''(z) = V_0(1-2a\delta(z))$. In (63) we introduced the factor γ in order that the eigenvalues ω_p have the units of frequencies. We can construct a set of eigenfunctions $f_p(x)$ which satisfy (63) with the proper boundary conditions and which are orthonormal with respect to the scalar product (40). Construction of this eigenfunctions and the resulting spectra of eigenvalues ω_p are discussed in detail in Appendix A. For the critical nucleus the spectrum $\omega_{n,p}$ is given by (A.20), for the straight polymer we arrive at the spectrum $\omega_{s,p}$ given by (A.10). The most important features of these spectra are as follows. The fluctuation spectrum of the straight configuration consists of stable modes with $\omega_{s,p} \geq V_0/\gamma > 0$ for all modes $p \geq 0$. It is discrete for finite L and approaches a continuous spectrum in the thermodynamic limit of infinite L. On the other hand, the critical nucleus has a mixed fluctuation spectrum also in the thermodynamic limit.

The discrete part of the spectrum contains one unstable mode $\omega_{n,0} < 0$ that corresponds to a mode that is pulling the polymer further into the energetically favorable potential well. Furthermore, there is one zero translational mode of the nucleus with $\omega_{n,1} = 0$. Additionally, there are modes with $\omega_{n,p} \geq V_0/\gamma > 0$ for $p \geq 2$ that form a discrete spectrum for finite L and approach a continuum in the thermodynamic limit of infinite L. Numerical results for the spectrum of eigenmodes of the critical nucleus as a function of the force are shown in Figure 9.

In terms of the eigenvalues $\omega_{s,p}$ and $\omega_{n,p}$ at the straight configuration $z_q(x) = z_{\min}^-$ and the critical nucleus configuration $z_n(x)$, respectively, the energy expansions (62) can be written as

$$\mathcal{H}\{z(x)\} \approx E_s + \frac{\gamma r}{2}\sum_p {X_p}^2 \omega_{s,p}, \tag{64}$$

$$\mathcal{H}\{z(x)\} \approx E_s + \Delta E_n + \frac{\gamma r}{2}\sum_p {X_p}^2 \omega_{n,p} \tag{65}$$

with r from (40) and $E_s \equiv \mathcal{H}\{z_{\min}^-\}$.

9.3 Nucleation rate

Now we can calculate the nucleation rate j including the prefactors in (61) using Kramers theory for sufficiently large forces F. Although the derivation is analogous to previous approaches for elastic strings [6,7,10,11], we include it in order to make the paper self-contained.

We start from the Fokker-Planck equation for the time-dependent probability $P(\{\zeta(x)\},t)$ to find the polymer in configuration $\zeta(x)$,

$$P(\{\zeta(x)\},t) = \left\langle \prod_x \delta[\zeta(x) - z(x,t)] \right\rangle , \tag{66}$$

where $z(x,t)$ is a solution of the the Langevin equation (8). Then $P(\{z(\tilde{x})\},t)$ fulfills the Fokker-Planck equation [36]

$$\frac{\partial P(\{z(\tilde{x})\},t)}{\partial t} + \int \mathrm{d}x \frac{\delta J(x,\{z(\tilde{x})\},t)}{\delta z(x)} = 0\,, \tag{67}$$

where $J(x,\{z(\tilde{x})\})$ is the corresponding probability current in the configurational space at configuration $z(\tilde{x})$ and in the direction of $J(x,.)$. This probability current is given by

$$J(x,\{z(\tilde{x})\},t) = -\frac{1}{\gamma}\left(\frac{\delta\mathcal{H}}{\delta z(x)} + T\frac{\delta}{\delta z(x)}\right) P(\{z(\tilde{x})\},t)\,. \tag{68}$$

At low temperatures $\Delta E_n \gg T$ the polymer lies in the local metastable minimum and the rate of escape is small. Therefore $J \approx 0$, and the probability in (68) approximately has the form of the stationary equilibrium distribution

$$P_{\mathrm{eq}}(\{z(x)\}) = \frac{1}{Z_s}\exp(-\mathcal{H}\{z(x)\}/T), \tag{69}$$

where the normalization factor is the partition sum $Z_s = \int \mathcal{D}z(x)\exp(-\mathcal{H}\{z(x)\}/T)$, where we integrate over configurations within the energy valley of the metastable minimum of the straight configuration. Using the expansion (64) we obtain

$$Z_s = e^{-E_s/T}\prod_{p\geq 0}\left(\frac{2\pi T}{\gamma r \omega_{s,p}}\right)^{1/2} \equiv e^{-E_s/T}\tilde{Z}_s\,. \tag{70}$$

In the presence of a driving force the system is out of equilibrium, and we make an Ansatz for the stationary state which includes a correction function $\hat{P}(\{z(x)\})$

$$P(\{z(x)\}) = \hat{P}(\{z(x)\})P_{\rm eq}(\{z(x)\}) \tag{71}$$

such that $\hat{P}(\{z_s\}) = 1$. Substituting (71) into (68), we get

$$J(x,\{z(\tilde{x})\}) = -\frac{T}{\gamma}\frac{\delta\hat{P}(\{z(\tilde{x})\})}{\delta z(x)}P_{\rm eq}(\{z(x)\})\ . \tag{72}$$

Now we consider the vicinity of the critical nucleus saddle configuration $z_n(x)$ and switch to a description of the configurational space by the appropriate normal modes using the decomposition $z(x) = z_n(x) + \sum_p X_p f_p(x)$. Each configuration $z(x)$ is specified by the set $\{X_a\}$ of expansion coefficients. We also decompose the current into the normal components according to

$$J(x,\{z(\tilde{x})\}) = \sum_p J_p(\{X_a\})f_p(x) \tag{73}$$

and transform functional derivatives according to $\delta/\delta z(x) = r^{-1}\sum_p f_p(x)\partial/\partial X_p$. Then, at the critical nucleus configuration $z_n(x)$ the components J_p of the current have the form

$$J_p(\{X_a\}) = -\frac{T}{\tilde{Z}_s\gamma r}\frac{\partial\hat{P}}{\partial X_p}\exp\left(-\frac{\Delta E_n}{T} - \frac{\gamma r}{2T}\sum_a X_a^2\omega_{n,a}\right), \tag{74}$$

where we used the quadratic approximation (65). It is assumed that the nucleation process proceeds along the unstable mode $p = 0$ such that we have a non-vanishing current only in this direction, $J_0(\{X_a\}) \neq 0$. In all other directions the system can equilibrate such that $J_p(\{X_a\}) = 0$ for $p > 0$. Then, according to (74), $\hat{P} = \hat{P}(X_0)$ is a function of X_0 only, such that corrections to the equilibrium in (71) only occur in the coordinate of the unstable mode carrying the system over the saddle. Moreover, according to (67), in a stationary state J has to fulfill the zero-divergence condition

$$0 = \int {\rm d}x\frac{\delta J(x,\{z(\tilde{x})\},t)}{\delta z(x)} = \sum_p\frac{\partial J_p(\{X_a\})}{\partial X_p} = \frac{\partial J_0(\{X_a\})}{\partial X_0}, \tag{75}$$

i.e., the only non-zero current component $J_0 = J_0(\{X_{a>0}\})$ does not depend on X_0.

Then, we can integrate (74) along the "reaction coordinate" X_0 to obtain $\hat{P}(X_0)$:

$$\hat{P}(X_0) = 1 - \frac{\tilde{Z}_s\gamma r}{T}J_0(\{X_{a>0}\})\int_{X_{0,i}}^{X_0}{\rm d}\tilde{X}_0 \times\exp\left(\frac{\Delta E_n}{T} - \frac{\gamma r}{2T}\tilde{X}_0^2|\omega_{n,0}| + \frac{\gamma r}{2T}\sum_{p>0}X_p^2\omega_{n,p}\right). \tag{76}$$

Starting from the nucleus configuration $X_0 = 0$, we reach the initial straight equilibrium configuration at some $X_{0,i} < 0$. There, we have the boundary condition $\hat{P}(X_{0,i}) = 1$, see (71). On the other hand, at positive values of X_0, kink-antikink formation takes place. We assume that the force is sufficiently high that kink and antikink are quickly driven apart, and we can assume a sink with $\hat{P}(X_{0,f}) = 0$ at some final $X_{0,f} > 0$. Using also this second boundary condition in (76), we obtain the current from (76),

$$J_0(\{X_{a>0}\}) = I\exp\left(-\frac{\gamma r}{2T}\sum_{p>0}X_p^2\omega_{n,p}\right) \tag{77}$$

with a constant I that is given by

$$\begin{aligned} I &= \frac{T}{\tilde{Z}_s\gamma r}\left[\int_{X_{0,i}}^{X_{0,f}}{\rm d}\tilde{X}_0\exp\left(\frac{\Delta E_n}{T} - \frac{\gamma r}{2T}\tilde{X}_0^2|\omega_{n,0}|\right)\right]^{-1} \\ &= \frac{T}{\tilde{Z}_s\gamma r}\left(\frac{\gamma r|\omega_{n,0}|}{2\pi T}\right)^{1/2}\exp\left(-\frac{\Delta E_n}{T}\right). \end{aligned} \tag{78}$$

Integration of equation (77) over all coordinates $X_{a>0}$ and division by the length $L + L'$ of the polymer yield the total nucleation current per length

$$\begin{aligned} j &\equiv \frac{1}{L+L'}\left(\prod_{a>0}{\rm d}X_a\right)J_0(\{X_{a>0}\}) \\ &= G\frac{1}{2\pi}\left(\frac{\gamma r}{2\pi T}\right)^{1/2}Q_n\exp\left(-\frac{\Delta E_n}{T}\right), \end{aligned} \tag{79}$$

where we used (70) and $Q_n^2 \equiv |\omega_{n,0}|\omega_{s,0}\omega_{s,1}\prod_{p>1}\times(\omega_{s,p}/\omega_{n,p})$ is given by the ratio of the products of all attempt frequencies, which have to be taken for straight and nucleus configurations of the same length $L + L'$. Using results from Appendix A, we find

$$Q_n^2 \approx \left|1 - 2^{4/3}\left(1 - \frac{F}{F_c}\right)^{-8/3}\right|\left(\frac{V_0}{\gamma}\right)^3 \tag{80}$$

as the force F approaches the critical force F_c, and for forces $F \ll F_c$ the factor Q_n shows a linear force dependence

$$Q_n^2 \approx \frac{16}{3}\frac{F}{F_c}\left(\frac{V_0}{\gamma}\right)^3\ . \tag{81}$$

The factor $G \equiv (\int {\rm d}X_1)/(L+L')$ in (79) is the result of the integration $\int {\rm d}X_1$ over the zero translational mode and the division by the polymer length. G can be calculated by noting that the zero translational mode is given by $f_1(x) = \alpha\partial_x z_n$, where α is determined by normalization with the scalar product (40) according to $\langle f_1|f_1\rangle = 1$, which gives $1/\alpha^2 = r^{-1}\int {\rm d}x(\partial_x z_n)^2$. Then, we can use the identity $z_n(x+\Delta x) = z_n(x) + \Delta x\partial_x z_n$ to relate $X_1 = \Delta x/\alpha$ to the displacement coordinate Δx of the nucleus, which we can conveniently integrate over the whole length $L + L'$ of the polymer to obtain

$$G = \frac{1}{L+L'}\int {\rm d}X_1 = \frac{1}{\alpha} = r^{-1/2}\left[\int {\rm d}x(\partial_x z_n)^2\right]^{1/2}\ . \tag{82}$$

Close to the critical force the factor G vanishes as

$$G \approx w_k^{-1} \left(1 - \frac{F}{F_c}\right) , \tag{83}$$

whereas we find

$$G \approx w_k^{-1} \left(3 - 6\frac{F}{F_c} + 2\frac{F}{F_c} \ln\left(\frac{\sqrt{2}F}{F_c}\right)\right)^{1/2} \tag{84}$$

for forces $F \ll F_c$.

9.4 Steady-state density and small force regimes

In the previous section we have found the nucleation rate (79) in the regime of sufficiently strong forces $F > F_{\rm cr}$ [35], with a crossover force $F_{\rm cr}$ given by

$$F_{\rm cr} \equiv \frac{T}{2aw_k} = \frac{F_c T}{E_k} . \tag{85}$$

The sink approximation for the upper integration boundary in (78) does not apply for weak forces $F < F_{\rm cr}$; then the mechanical energy, $|\mathcal{F}_k| w_k = 2aFw_k$ (see Eq. (20)), required for pulling an isolated kink through a distance of the kink width w_k is less than the thermal energy stored in the nucleating pair, *i.e.*, $\mathcal{F}_k w_k < T$ or $F < F_{\rm cr}$. In this regime the nucleus attains a broad quasi-equilibrium configuration before kink and antikink are driven apart. This quasi-equilibrium configuration resembles a weakly perturbed kink-antikink pair, which has *two* zero translational modes, as worked out in Appendix A. These correspond to a translation of the kink-antikink pair and a "breathing" mode leading to relative displacement of kink and antikink. Existence of two soft modes makes the calculation of the previous section inapplicable.

Comparing the two crossover forces $F_{\rm cr}$ given by (85) and $F_\rho = T\rho/a$ from (50), we realize that $F_{\rm cr} \gg F_\rho$ as long as kinks do not overlap, *i.e.*, for $\rho \ll 1/2w_k$, which is always fulfilled in the regime $E_k \gg T$ of thermally activated behaviour that we focus on. Therefore, we have $F \gg F_{\rm cr} \gg F_\rho$ and use expression (51) to obtain the steady-state density

$$\rho = \left(\frac{j}{2v}\right)^{1/2} , \qquad \text{for } F \gg F_{\rm cr}, \tag{86}$$

from the result (79) for large forces.

In the regime $F < F_{\rm cr}$ we can use a quasi-equilibrium approximation based on the energy (59) of the nucleus at small forces [6,7,35], where it can be approximated by a kink-antikink pair. According to reference [5], in equilibrium the kink number on a polymer of length L is given by $\rho_{\rm eq} L = Z_n/Z_s$, *i.e.*, the ratio of the partition function Z_n of a polymer with one kink and Z_s of a straight, kinkless polymer as given by (70). Note that in both configurations the total length of the polymer should be $(L + L')/2 \approx L$. Using the result (59) for the energy of the nucleus at small forces, which represents kink *and* antikink, the quasi-equilibrium approximation gives

$$\rho = \frac{2}{L + L'} \frac{\tilde{Z}_n}{\tilde{Z}_s} \exp\left(-\frac{\Delta E_n}{2T}\right) \tag{87}$$

with $\tilde{Z}_s$ from (70) and $\tilde{Z}_n$ as the partition function of the fluctuations around the kinked state

$$\begin{aligned} \tilde{Z}_n &= \left(\prod_{p \text{ odd}} \int \mathrm{d}X_p\right) \exp\left(-\frac{\gamma r}{2T} \sum_p {X_p}^2 \omega_{n,p}\right) \\ &= \frac{L + L'}{2} \frac{G}{\sqrt{2}} \prod_{p>1,\ \text{odd}} \left(\frac{2\pi T}{\gamma r \omega_{n,p}}\right)^{1/2} , \end{aligned} \tag{88}$$

where we take only the odd eigenfrequencies $\omega_{n,p}$ of the critical nucleus at small forces as the single kink has half the length and symmetric even modes are not possible. The factor $G/\sqrt{2}$ given by the small force limit (83) is the result of the integration over the zero translational mode of a single kink on a polymer of length $(L + L')/2$. Then, (87) leads to

$$\rho = G \left(\frac{\gamma r}{4\pi T}\right)^{1/2} \tilde{Q}_n \exp\left(-\frac{\Delta E_n}{2T}\right) , \tag{89}$$

where $\tilde{Q}_n^2 \equiv \omega_{s,0} \prod_{p>0} (\omega_{s,p}/\omega_{n,2p+1}) \approx V_0/\gamma$.

For small driving forces $F = 0$ the system reaches thermodynamic equilibrium, $\rho(F = 0) = \rho_{\rm eq}$. In this limit the nucleus approaches a kink-antikink pair of energy $2E_k$. Accordingly, the eigenfrequencies $\omega_{n,p}$ approach those of a kink-antikink pair as worked out in Appendix A. Then, $\tilde{Q}_n$ approaches $\tilde{Q}_k^2 \equiv \omega_{s,0} \prod_{p>0} (\omega_{s,p}/\omega_{k,p}) \approx V_0/\gamma$. Using (84) we also find $G = \sqrt{3}/w_k$. For $F = 0$ the result (89) then reduces to

$$\rho_{\rm eq} = \sqrt{\frac{3}{w_k}} \left(\frac{\gamma}{4\pi T}\right)^{1/2} \tilde{Q}_k e^{-E_k/T} \approx \sqrt{\frac{3}{2\pi}} \frac{1}{w_k} \sqrt{\frac{E_k}{T}} e^{-E_k/T} . \tag{90}$$

For intermediate forces $F_\rho \ll F < F_{\rm cr}$, the nucleation current can be obtained by inserting equation (89) into the relation $j = 2v\rho^2$, see (51). For very small forces $F \ll F_\rho$, we insert (89) or (90) into the corresponding relation $j = 4D_k\rho^3$ for diffusion-dominated behaviour, see (52). Having derived the steady-state kink density ρ as a function of the material parameters of the semiflexible polymer in all regimes, the defining relation (50) for the crossover force F_ρ becomes a self-consistent relation

$$F_\rho = \frac{T}{a} \rho(F_\rho) \tag{91}$$

from which the actual value for F_ρ has to be obtained.

Finally, for $\rho < 1/L$, where L is the total length of the polymer, the finite-size effects dominate and we cross over to single-kink behaviour, *i.e.*, the barrier crossing proceeds by creation of a single kink and its motion to the ends of the polymer as described in Section 7. This regime is reached for small forces $F < F_L$ where F_L is determined by $\rho(F) = 1/L$ using (89).

9.5 Longitudinal motion

Fluctuations in the z-coordinate as described by the equation of motion (8) require fluctuations of the contour length L_c and thus longitudinal motion of polymer segments in the x-direction if the filament is inextensible [28–32]. So far, we implicitly assumed that the longitudinal dynamics is much faster than the activated dynamics in the z-direction. In this section we discuss the validity of this assumption in more detail.

First, we point out that *after* the creation of a kink its dynamical properties are independent of the longitudinal friction because the motion of a kink does not require the longitudinal motion of polymer segments as the contour length is preserved. Therefore, effects from longitudinal friction do not affect the dynamical behaviour of a single moving kink as discussed in Section 5.

In principle, longitudinal friction effects could affect the kink nucleation which requires an excess contour length. However, kink nucleation is an activated process and thus exponentially slow in the regime $T \ll \Delta E_n$ according to the Arrhenius law (61). Therefore, longitudinal friction is relevant only for driving forces F close to the critical force F_c. Specifically, the nucleation of a single kink-antikink pair in a straight polymer requires an excess contour length of $\Delta L_{c,k} = 3a^2/2w_k$ which can be generated by thermal fluctuations within a single valley of the external potential. In the absence of an external potential transverse fluctuations scale as $\langle z^2(t)\rangle \propto t^{1/4}$ and longitudinal fluctuations of the contour length as $\langle \delta L_c(t)^2\rangle \propto t^{7/8}$ [28–32]. In the presence of an external potential, segments are only correlated over a finite length $\sim x_{\rm sc} = (\kappa/V_0)^{1/4}$, see equation (6), and each segment of length $x_{\rm sc}$ relaxes within a finite time $\sim t_{\rm sc} = \gamma/V_0$ as the scaling analysis in Section 2 shows, see equation (10). Following the arguments of reference [29] to correctly take into account longitudinal friction effects, this leads to finite transverse fluctuations $\langle z^2(t)\rangle \sim x_{\rm sc}^3/L_p$ and longitudinal fluctuations $\langle \delta L_c(t)^2\rangle \sim (Tt/\gamma)^{1/2} x_{\rm sc}^{3/2}/L_p$ (assuming an isotropic damping constant γ). The condition $\langle \delta L_c(t_\parallel)^2\rangle = (\Delta L_{c,k})^2$ estimates the time $t_\parallel$ necessary to generate the excess contour length for a kink-antikink pair by thermal fluctuations against the longitudinal friction. As long as this time scale is small compared to the exponentially large nucleation time, *i.e.*, $t_\parallel \ll 1/Lj \propto \exp \Delta E_n/T$, longitudinal friction does not affect nucleation of a *single* kink-antikink. The effect of longitudinal friction on the nucleation of a single kink-antikink for driving forces close to the critical force F_c remains an interesting problem for future research.

In the stationary state of the driven system *many* kink-antikink pairs are present with a density ρ and in a dynamical equilibrium between kink production and kink annihilation. In this stationary state excess contour length does not have to be created by thermal fluctuations but only *transported* over typical distances $\sim 1/\rho$ between creation and annihilation events such that the total contour length stays constant in the stationary state. Excess contour length can be transported by reptation-like motion which requires only transversal displacements of polymer segments (the characteristic velocity for this transport is $\sim v_{\rm sc} = x_{\rm sc}/t_{\rm sc}$, see Eq. (11), which is comparable to the kink velocity). Therefore, we do not expect that longitudinal friction effects change the dynamical stationary state of the driven system.

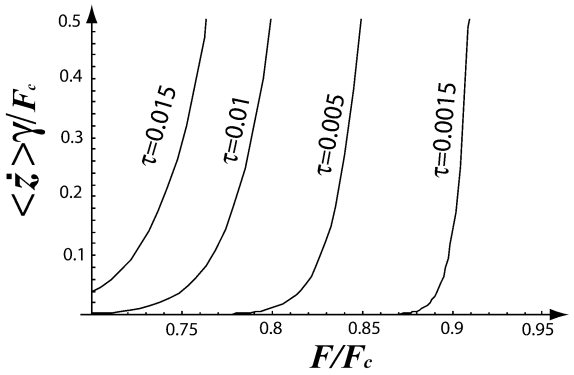

Fig. 10. Average angular velocity $\langle \partial_t z\rangle$ (in units of $aV_0/\gamma = F_c/\gamma$) of the semiflexible polymer as a function of the force F/F_c for different rescaled temperatures $\tau = T/E_k$, $\tau = 0.0015$, $\tau = 0.005$, $\tau = 0.01$, $\tau = 0.015$.

10 Mean polymer velocity

The average velocity of the semiflexible polymer is given by $\langle \partial_t z\rangle = 4av\rho$ in terms of the kink (antikink) density ρ and the kink velocity v. At a given point $2v\rho$ kink and antikinks pass per time, each giving rise to a displacement $2a$.

For large forces $F > F_{\rm cr}$ the equation (86) leads to an average polymer velocity $\langle \partial_t z\rangle = 2a(2vj)^{1/2}$ [10] with j given by expression (79). The propagation velocity $v(F)$ depends on the force F as shown in Figure 5. For forces F close to the critical force F_c the velocity diverges as $v \sim (1 - F/F_c)^{-3/2}$. Introducing the rescaled temperature $\tau \equiv T/E_k$ (with $\tau \ll 1$ in the regime of thermally activated behaviour that we focus on) we find the force dependence of the rescaled average angular velocity $\langle \partial_t z\rangle \gamma/aV_0$ as shown in Figure 10.

In the regime of intermediate driving forces $F_\rho \ll F < F_{\rm cr}$, the critical nucleus is in quasi-equilibrium and the angular velocity $\langle \partial_t z\rangle = 4av\rho$ contains the density (89). For small driving forces $F \ll F_\rho$ the kink motion is purely diffusive, and the system reaches thermodynamic equilibrium with a kink density $\rho_{\rm eq}$ given by the Boltzmann distribution (90) and with $\langle \partial_t z\rangle = 4av\rho_{\rm eq}$. Equation (90) gives for the average velocity the following expression:

$$\langle \partial_t z\rangle = 4\sqrt{\frac{3}{2\pi}}\frac{av}{w_k}\sqrt{\frac{1}{\tau}}\exp\left(-\frac{1}{\tau}\right). \qquad (92)$$

At low fields the propagation velocity has a linear force dependence with $av/w_k \approx 4F/\gamma$ as follows from (30) and (31). Therefore, the angular velocity increases linearly with force.

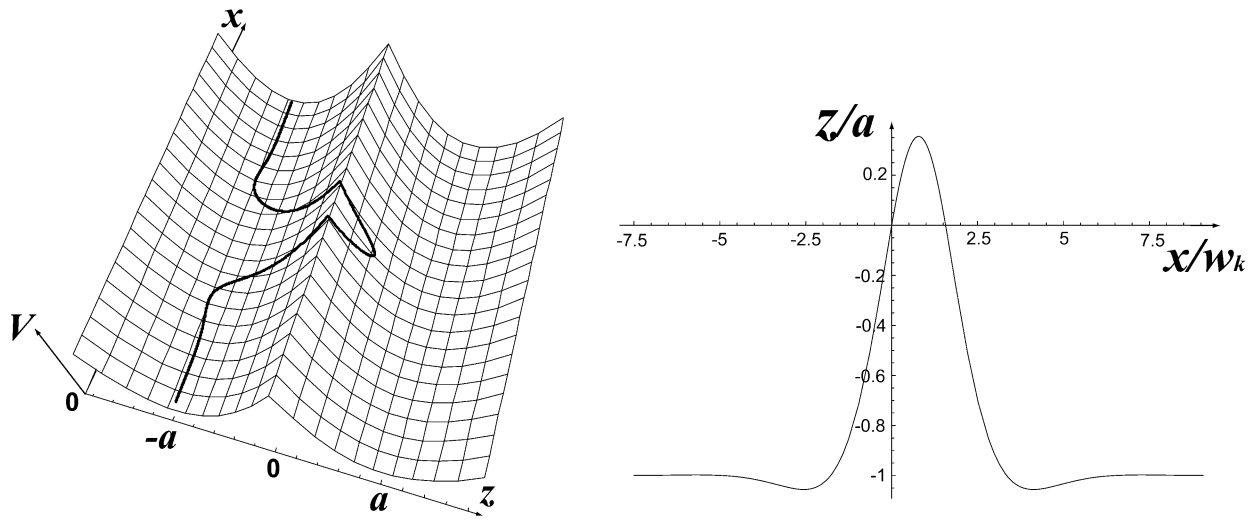

Fig. 11. Left: Semiflexible polymer in a static kink-like configuration in a double-well potential $V_s(z)$ and under the influence of a point force F_p acting at the midpoint. Right: Polymer displacement z (in units of a) as a function of x (in units of w_k) for the same kink-like configuration as shown on the left. The point force is $F_p = 2.6 \times 10^{-4} F_{p,c}$, the equilibrium displacement of the middle point is $z_m/a \approx 0.35$. The total length of the polymer is $L = L_1 + L_2$. For $L_1 = 15 w_k$ we find $L_2 \approx 1.57 w_k$ for the distance between the points where the potential barrier is crossed.

11 Point forces

Advances in the manipulation techniques of polymers allow the experimentalist to study and visualize the motion of semiflexible polymers under the influence of external forces. On the experimental side micro-manipulation techniques using optical tweezers [37], AFM tips [23], or micropipettes [38] have become available to study the effect of external forces on semiflexible polymers. However, these modern manipulation techniques only allow the application of *point* forces. In this section we investigate the static metastable configurations of a semiflexible polymer under the influence of an external point force F_p acting on the polymer. A complete description of the activated dynamics under the influence of point driving forces will be given elsewhere [39].

The Hamiltonian in the presence of a point force is similar to (2) but contains a potential

$$V_p(x,z) \equiv V_s(z) - F_p \delta(x - x_p) z \; . \tag{93}$$

$V_s(z) \equiv \frac{1}{2} V_0 (|z| - a)^2$ is the symmetric harmonic double-well potential and the last term contains the action of a point force of strength F_p acting at $x = x_p$. Note that the point force in (93) breaks the translational invariance of the system in the x-direction. The resulting Hamiltonian for a polymer of length L can be written as

$$\mathcal{H} = \int_L \mathrm{d}x \left[\frac{\kappa}{2} \left(\partial_x^2 z \right)^2 + \frac{1}{2} V_0 (z + a)^2 \right] - F_p z \left(x_p \right) . \tag{94}$$

The overdamped dynamics of the polymer is described by the equation of motion

$$\begin{aligned} \gamma \partial_t z &= -\frac{\delta \mathcal{H}}{\delta z} + \zeta(x,t) \\ &= -\kappa \partial_x^4 z - V_s'(z) + F_p \delta(x - x_p) + \zeta(x,t), \end{aligned} \tag{95}$$

with the damping constant γ and thermal noise $\zeta(x,t)$ with correlations (9).

We want to calculate the stationary shape of a polymer that is deformed by the action of the point force acting at the midpoint of the polymer into a "restricted" kink-antikink configuration $z_{kp}(x)$ as shown in Figure 11. This configuration is obtained by solving the saddle point equation $\delta \mathcal{H}/\delta z = 0$ for the energy (94), which is equation (95) for the time-independent case and in the absence of noise ($\zeta = 0$),

$$\begin{aligned} &\kappa \partial_x^4 z + V_0 (z + a) + F_p \delta(x - x_p) = 0, \quad \text{for } z < 0, \\ &\kappa \partial_x^4 z + V_0 (z - a) + F_p \delta(x - x_p) = 0, \quad \text{for } z > 0. \end{aligned} \tag{96}$$

For $z(x_p) > 0$ the kink configuration crosses the barrier at two points, see Figure 11; we choose the origin $x = 0$ and the length L_2 such that these points are $z_{kp}(0) = 0$ and $z_{kp}(L_2) = 0$. The polymer has a total length $L = L_1 + L_2$ and extends from $x = -L_1/2$ to $x = L_1/2 + L_2$, and the force acts at the midpoint $x_p = L_2/2$. We introduce four parts of the solution separated by the two crossing points and the midpoint: $z_{kp1+}(x)$ and $z_{kp2+}(x)$ in regions $0 < x < L_2/2$ and $L_2/2 < x < L_2$, respectively, where $z > 0$; $z_{kp1-}(x)$ and $z_{kp2-}(x)$ in regions $-L_1/2 < x < 0$ and $L_2 < x < L_1/2 + L_2$, respectively, where $z < 0$. By introducing only two lengths L_1 and L_2 to describe four regions we used already that the configuration is symmetric with respect to the midpoint $x_p = L_2/2$. Away from the point force, *i.e.*, for $x \neq x_p$ the saddle point equation (96) is identical to (13) for static kinks in the absence of a force and thus each of the functions $z_{kpj\pm}$ ($j = 1, 2$) can be written in the following form:

$$\begin{aligned} z_{kp\pm j}(x) &= C_{1j\pm} \cos(\bar{x}) \cosh(\bar{x}) + C_{2j\pm} \sin(\bar{x}) \cosh(\bar{x}) \\ &+ C_{3j\pm} \cos(\bar{x}) \sinh(\bar{x}) + C_{4j\pm} \sin(\bar{x}) \sinh(\bar{x}) \pm a, \end{aligned} \tag{97}$$

where $\bar{x} = x/w_k$ and $C_{ij\pm}(i = 1,\ldots,4)$ are sixteen linear expansion coefficients. The kink-like configuration has to fulfill four boundary conditions $z_{kp}(-L_1/2) = z_{kp}(-L_1/2+L_2) = -a$ and $\partial_x z_{kp}|_{-L_1/2} = \partial_x z_{kp}|_{-L_1/2+L_2} = 0$. We also prescribe the displacement z_m of the polymer at the midpoint by $z_{kp}(L_2/2) = z_m$. At the midpoint $x_p = L_2/2$, the point force in (96) causes a discontinuity in the third derivative, $z'''_{kp2+}(L_2/2) - z'''_{kp1+}(L_2/2) = F_p/\kappa$. Additionally, we have four matching conditions $z_{kp1+}(L_2/2) = z_{kp2+}(L_2/2) = z_m$, $\partial_x^m z_{kp1+}|_{x=L_2/2} = \partial_x^m z_{kp2+}|_{x=L_2/2}$ for $m = 1,2$. We also have ten matching conditions $z_{kp1-}(0) = z_{kp1+}(0) = 0$, $\partial_x^m z_{kp1-}|_{x=0} = \partial_x^m z_{kp1+}|_{x=0}$ and $z_{kp2-}(L_2) = z_{kp2+}(L_2) = 0$, $\partial_x^m z_{kp2-}|_{x=L_2} = \partial_x^m z_{kp2+}|_{x=L_2}$ for $m = 1,2,3$ at the two crossing points $x = 0, L_2$. Only eight of these matching conditions are independent due to the symmetry around the midpoint. Therefore, we have 17 independent boundary and matching conditions for 16 unknown linear expansion coefficients and 2 unknown parameters L_2 and z_m. Using also $L = L_1 + L_2$, we can thus determine all parameters as a function of the system size L and the remaining model parameters, in particular the the point force F_p. As a result of this procedure we can obtain the shape of the kink-like configuration for $z_m > 0$ as shown in Figure 11. For $z_m = a$ and $F_p = 0$ the configuration approaches a static kink-antikink pair.

For $z_m < 0$ the solution does not cross the potential barrier such that we can set $L_2 = 0$ and we only need to introduce two parts of the solution separated by the midpoint which is then located at $x_p = 0$: $z_{kp1-}(x)$ and $z_{kp2-}(x)$ in regions $-L_1/2 < x < 0$ and $0 < x < L_1/2$, respectively, with $z < 0$ in both regions. The point force in (96) causes a discontinuity in the third derivative at $x_p = 0$, $z'''_{kp2-}(0) - z'''_{kp1-}(0) = F_p/\kappa$, whereas lower derivatives have to match and $z_{kp1-}(0) = z_{kp2-}(0) = z_m$. Then, we have 4 boundary and 5 matching conditions to determine 8 unknown linear expansion coefficients and the unknown parameter z_m as a function of the system size $L = L_1$ and the remaining model parameters including the point force F_p.

The above construction also allows to determine the position of the midpoint of the polymer as a function of the external force $z_m(F_p)$, which is shown in Figure 12. For $z_m < 0$ and in the limit of large $L \gg w_k$ we find the linear relation

$$z_m = a\left(-1 + \frac{F_p a}{4E_k}\right) . \tag{98}$$

For $z_m > 0$ in the limit of large $L \gg w_k$, on the other hand, we can derive the following set of two equations for the position of the middle point z_m and the length L_2:

$$\frac{F_p a}{4E_k} = [\cos(L_2/2w_k) - \sin(L_2/2w_k)]\, e^{-L_2/2w_k}, \tag{99}$$

$$z_m = a[1 - e^{-L_2/2w_k}(\sin(L_2/2w_k) + \cos(L_2/2w_k))]. \tag{100}$$

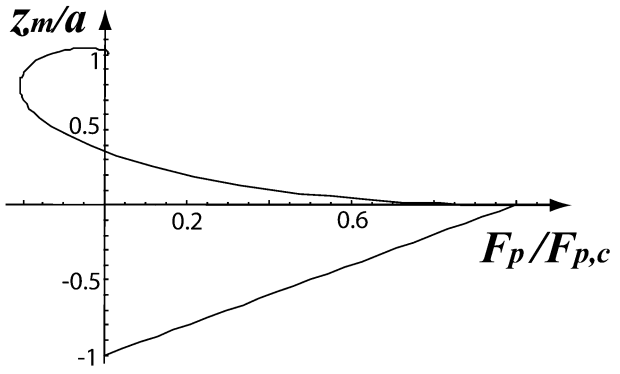

Fig. 12. The middle point z_m (in units of a) in a kink-like polymer configuration as a function of the external force (in units of the critical force $F_{p,c} = 4E_k/a$).

Solving (100), we find the midpoint of the polymer as a function of the external force $z_m(F_p)$ for $z_m > 0$, which is shown in Figure 12 together with the linear result (98) for $z_m < 0$. As one sees from (98) and (99), there are no solutions $z_m < a$ to equation (99) if the force F_p exceeds a critical value $F_{p,c}$ given by

$$F_{p,c} \equiv 2\sqrt{2}a\kappa^{1/4}V_0^{3/4} = \frac{4E_k}{a}. \tag{101}$$

Therefore, there exists no stationary states for $F > F_{p,c}$ above the critical point force $F_{p,c}$, and the polymer spontaneously crosses the barrier to values $z_m > a$. $F_{p,c}$ is the analogon of the uniform critical force F_c. We note that the measurement of the critical point force $F_{p,c}$ allows to determine the single-kink energy E_k according to (101) if the distance $2a$ between the two potential minima is known.

The function $z_m(F_p)$ is multivalued for $0 < F_p < F_{p,c}$ as can be seen from Figure 12. By prescribing z_m in our construction of stationary configurations $z_{kp}(x)$, we also obtain saddle point configurations which can be unstable with respect to fluctuations displacing the midpoint. Therefore, we also obtain the critical nucleus configuration for a given point force F_p using the above procedure. The higher value $z_m(F_p)$ represents the critical nucleus configuration which is indeed locally unstable as $z_m(F_p)$ is increasing with decreasing F_p and already a *smaller* force would suffice to pull the polymer to larger z_m. When the midpoint of the polymer is displaced beyond a critical value, we even find negative values of F_p and the polymer will be pulled to larger z_m spontaneously even in the absence of a point force. The critical value for z_m agrees with the position of the maximum in the kink-antikink bending energy in Figure 3. After crossing this energy barrier, the polymer can move spontaneously at $F_p = 0$ into the stable static kink-antikink configuration that is reached for $z_m = a$ and $F_p = 0$.

Table 1. List of symbols.

κ	bending rigidity	
L_p	persistence length	equation (1)
T	temperature in energy units	equation (1)
$z(x)$	polymer displacement	equation (2)
x	coordinate parallel to potential well	
$V(z)$	surface potential	equation (3)
V_0	potential strength	equation (3)
F	uniform driving force	equation (3)
a	half distance between potential minima	equation (3)
F_c	critical force	equation (4)
$E_{\rm sc}$	characteristic energy	equation (5)
$x_{\rm sc}$	characteristic length	equation (6)
$t_{\rm sc}$	characteristic time	equation (10)
$v_{\rm sc}$	characteristic velocity	equation (11)
γ	damping constant	equation(8)
$\zeta(x,t)$	thermal noise	equation(9)
w_k	kink width	equations (14, 25)
E_k	kink energy	equation (18)
v	kink velocity	
y	x-coordinate in comoving kink frame	
η_k	kink friction constant	
$E_{\rm int}$	kink-antikink interaction energy	equation (19)
d	kink-antikink separation distance	equation (19)
L	kink length	
$\mathcal{F}_k$	kink driving force	equation (20)
$\mathcal{F}_f$	kink friction force	
$x_k(t)$	kink center position	
ϕ_p	normal modes	equation (34)
X_p	expansion coefficients	equation (34)
f_p	eigenfunctions	equation (39)
ω_p	eigenvalues	equation (39)
$\langle .\vert .\rangle$	scalar product	equation (40)
r	dimensionful constant in scalar product	equation (40)
C	normalization constant	equation (42)
D_k	kink diffusion constant	equation (47)
$t_{\rm cr}$	average polymer crossing time	
$t_{\rm rel}$	polymer relaxation time	
ρ	kink density	
τ_F	average kink lifetime of a kink for large force F	
τ_D	average kink lifetime of a kink for small force F	
F_ρ	characteristic force	equation (50)
j	nucleation rate	equations (52, 51)
ΔE_n	excess energy of the critical nucleus	equation (56)
E_s	energy of straight state	
$\omega_{n,p}$	fluctuation spectrum of critical nucleus	
$\omega_{k,p}$	fluctuation spectrum of kink	
$\omega_{s,p}$	fluctuation spectrum of straight polymer	
$P(\{\zeta(x)\},t)$	probability to find the polymer in configuration $\zeta(x)$	equation (66)
J	probability current	equation (68)
J_p	components of probability current	equation (74)
$P_{\rm eq}$	equilibrium distribution	equation (69)
Z_s	partition sum of straight polymer	equation (70)
$\tilde{Z}_n$	partition function of the fluctuations around the kinked state	equation (88)
G	integral over the zero translational mode	
$F_{\rm cr}$	crossover force	equation (85)
$\rho_{\rm eq}$	equilibrium kink density	equation (90)
τ	rescaled temperature	equation (92)
$V_p(x,z)$	surface potential	equation (93)
F_p	point driving force	equation (93)
x_p	coordinate where point force acts	
z_m	midpoint displacement of polymer	equation (98)
$F_{p,c}$	critical point force	equation (101)

12 Experimental observables

The aim of this Section is to show how the theoretical results presented above can be used to analyze experimentally measurable observables in order to extract the material parameters characterizing the semiflexible polymer and the structured substrate. The conformational properties of polymers are specified by the bending rigidity κ or the persistence length L_p, which is the length beyond which tangent correlations fall off exponentially and is usually determined experimentally by measuring steady-state tangent correlation function using, *e.g.*, video microscopy. We want to demonstrate that experiments on the activated dynamics of semiflexible polymers on structured substrates not only provide an alternative way of measuring the persistence length L_p of the polymer but also allow to determine substrate parameters such as the barrier height V_0 or the distance $2a$ between potential minima. It might also be possible to infer the damping constant γ of the polymer which is related to the dynamics properties of the polymer.

Experimentally accessible quantities are i) the static kink width w_k, see (14) in the absence of a driving force, *e.g.*, by optical microscopy, ii) the critical uniform force F_c and iii) the critical point force $F_{p,c}$ below which the polymer starts to move spontaneously without activation energy. Eventually, also iv) the kink diffusion constant D_k can be measured by analyzing the diffusive relaxation of single kinks in the absence of a driving force. Measuring two of the three quantities i)–iii) is sufficient to obtain κ and V_0 if the half-distance a between potential minima is known:

$$\kappa = \frac{F_{p,c} w_k^3}{8a} = \frac{F_c w_k^4}{4a}\,,$$
$$V_0 = \frac{F_c}{a} = \frac{F_{p,c}}{2w_k a}\,. \qquad (102)$$

$F_c = V_0 a$, provides direct information about the barrier height V_0, and $F_{p,c} = 4E_k/a$, see (101), is directly related to the kink energy E_k.

If, additionally, the kink diffusion constant $D_k = T/\eta_k = 2Tw_k/3a^2\gamma$ in the absence of driving forces can be measured, we can additionally gain information on the damping constant of the semiflexible polymer, which characterizes its dynamical properties.

13 Conclusion

In conclusion, we described the activated dynamics of semiflexible polymers which is governed by kink excitations. We obtained the energy $E_k \sim a^2\kappa^{1/4}V_0^{3/4}$ of a static kink as well as its width $w_k \sim (\kappa/V_0)^{1/4}$. In the presence of a driving force F there is a force $\mathcal{F}_k$ acting on the kink that leads to moving kink solutions with a velocity $v(F)$ whose dependence on F we obtained in (29). In the absence of kink-phonon scattering the kink performs Brownian motion with drift, for which we have calculated the friction constant η_k and the diffusion constant D_k. This leads to estimates for the crossing times $t_{\rm cross} \sim L/F$ for $F > 2T/La$ and $t_{\rm cross} \sim L^2/T$ for small forces $F < 2T/La$. The nucleation of kinks proceeds by activation over the saddle point which is the critical nucleus. Application of Kramers theory allows to calculate the nucleation rates (79) at large forces, in quasi-equilibrium at small forces we can calculate the kink density (89) or (90). In all regimes the dynamical equilibrium of kink nucleation and annihilation allows to determine the average velocity of the polymer. We also investigated the static metastable configurations if a point force F_p is applied at the middle point of the semiflexible polymer. In this case spontaneous motion sets in above a critical force $F_{p,c} = 4E_k/a$.

In order to describe the activated dynamics of the semiflexible polymer we used the same general framework that has been derived for elastic strings [6,10,35], such as dislocation lines in crystals or flexible polymers. Also the activated dynamics of the semiflexible polymer is governed by the nucleation and motion of localized, kink-like excitations. However, there are important differences with respect to elastic strings or flexible polymers as the kink properties are not governed by entropic elasticity or tension of the polymer chain but rather by the bending energy of the semiflexible polymer. This leads to a number of differences, the most important of which are the distinct dependence of the kink width w_k and kink-energy E_k on the bending rigidity as calculated in (14) and (18). These dependencies enable us to determine the persistence length from kink properties using the relations (102). There are numerous other differences due to the bending-energy–dominated behaviour, for example, the peculiar non-monotonous kink shapes, see for example Figure 2 for a static kink. Not only static properties but also the dynamic behaviour of the semiflexible polymer is different as compared to a flexible polymer. We find characteristic differences in the force-velocity relation for a moving kink, the critical nucleus energy, and in the behaviour of fluctuation modes.

Appendix A. Fluctuation eigenmodes

In this appendix we analyze the eigenmode spectrum of fluctuations around all three types of local extrema of the energy (2), the critical nucleus $z_n(x)$, a resting single kink $z_k(x)$, and the kinkless straight state $z_s = z^-_{\rm min}$. The kink-antikink pair is a metastable configuration in the absence of force ($F = 0$). We analyze fluctuations of the critical nucleus configuration for uniform forces $F > 0$. The fluctuation spectrum of the straight configuration turns out to be force independent.

In the following, we denote the extremal configuration by $z_q(x)$ where q is a subscript q which can equal n, k, or s corresponding to the three types of local extrema of the energy (2), the critical nucleus (n), the static kink (k), and the straight state (s). Expansion of the energy in the neighborhood of a local extremum $z_q(x)$ up to second oder

in a perturbation $\delta z_q(x)$ yields

$$\mathcal{H}\{z_q(x)+\delta z_q(x)\} \approx \mathcal{H}\{z_q(x)\} + \frac{1}{2}\int \mathrm{d}x \delta z_q(x) \left[\kappa\partial_x^4 + V''(z_q(x))\right] \delta z_q(x), \quad \text{(A.1)}$$

where $V''(z) = V_0(1-2a\delta(z))$. Note that this result depends on the force only through the shape of the configuration $z_q(x)$. We expand the perturbations $\delta z_q(x)$ in terms of normal modes $\delta z_q(x) = \sum_p X_p f_p(x)$. The normal modes $f_p(x)$ are the orthogonal set of eigenfunctions for the set of eigenvalues ω_p of the linear eigenvalue equation

$$\kappa\partial_x^4 f + V''(z_q(x))f = \omega\gamma f \quad \text{(A.2)}$$

with $V''(z) = V_0(1-2a\delta(z))$, see (63).

For $z_q(x) \neq 0$, *i.e.*, away from the "cusp" of the potential the eigenfunction, $f(x)$ satisfies the eigenvalue equation

$$\kappa\partial_x^4 f = (\omega\gamma - V_0)f \ . \quad \text{(A.3)}$$

For $\omega \geq V_0/\gamma$ the general solutions of this equation are linear combinations of the four functions

$$f(x) = C_1\cos(x_-) + C_2\sin(x_-) + C_3\cosh(x_-) + C_4\sinh(x_-)\,, \quad \text{(A.4)}$$

where $x_- \equiv K_- x$ with

$$K_-^4 = |\omega\gamma - V_0|/\kappa \ . \quad \text{(A.5)}$$

For $\omega \leq V_0/\gamma$ they are linear combinations of the four functions

$$f(x) = C_1\cos(x^+)\cosh(x^+) + C_2\sin(x^+)\cosh(x^+) + C_3\cos(x^+)\sinh(x^+) + C_4\sin(x^+)\sinh(x^+), \quad \text{(A.6)}$$

where $x_+ \equiv K_+ x$ with

$$K_+^4 = |V_0 - \omega\gamma|/4\kappa \ . \quad \text{(A.7)}$$

The set of four linear expansion coefficients $C_i (i = 1,\ldots,4)$ has to be determined from boundary and matching conditions. The boundary conditions for the fluctuation modes are $f|_{\text{ends}} = 0$ and $f'|_{\text{ends}} = 0$ at both ends for all three types of configurations.

For the straight configuration we have to determine the 4 linear expansion coefficients from these 4 boundary conditions. The critical nucleus $z_n(x)$ and the kink $z_k(x)$ are piecewise defined as they cross the potential barrier at $z = 0$, the single kink once, and the critical nucleus twice, see Sections 3 and 9.1, respectively. The δ-function in (A.2) leads to discontinuities in the third derivative $f'''(x)$ across these crossing points. Therefore we introduce a piecewise definition of the eigenmodes $f(x)$ with up to three regions separated by the two points where the polymer crosses the barrier at $z = 0$. For each region we have a set of expansion coefficients C_i $(i = 1,\ldots,4)$ and at each crossing point we will get four additional matching conditions. For the kink, we have 8 expansion coefficient that are determined from 8 boundary and matching conditions, for the critical nucleus we have 12 expansion coefficients and 12 boundary and matching conditions. The resulting systems of linear equations for the determination of the expansion coefficients can only be solved for particular values of $K_\pm$ which leads to the spectrum of eigenvalues ω_p upon using (A.5) or (A.7).

Appendix A.1. Straight polymer (s)

For a straight polymer we have $z_s = z_{\min}^-$. The boundary conditions are $f(-L/2) = f(L/2) = 0$ and $f'(-L/2) = f'(L/2) = 0$ for a polymer of length L and we need 4 coefficients $C_i (i = 1,\ldots,4)$. The 4 boundary conditions lead to a homogeneous linear system of equations for 4 the coefficients C_i. The eigenvalues of (A.3) are found from the condition that the determinant of this homogeneous linear system of equations has to be zero.

For $\omega \leq V_0/\gamma$ we find only the trivial constant mode of the form (A.6) for $K_+ = 0$ with $\omega_{s,0} = V_0/\gamma$. Therefore, there are only eigenvalues $\omega \geq V_0/\gamma$ and solutions of the form (A.4), for which we find the condition

$$\tanh(K_-L/2) - \tan(K_-L/2) = 0 \quad \text{or} \quad \text{(A.8)}$$

$$\tanh(K_-L/2) + \tan(K_-L/2) = 0 \ . \quad \text{(A.9)}$$

The lowest eigenvalue is $\omega_{s,0} = V_0/\gamma$ corresponding to the root $K_- = 0$, *i.e.*, the constant mode. In the limit of large K_-L or large mode number p (A.8) and (A.9) lead to $\tan(K_-L/2) \approx \pm 1$. This gives solutions $K_-L \approx -\pi/2 + p\pi$ for $p \geq 1$, which become exact for large $p \gg 1$.

Finally, we obtain the spectrum

$$\omega_{s,0} = V_0/\gamma,$$
$$\omega_{s,p} \approx V_0/\gamma + \kappa\left[\left(-\frac{\pi}{2} + p\pi\right)/L\right]^4, \quad \text{for } p \geq 1, \quad \text{(A.10)}$$

which becomes exact for $p \gg 1$. In the limit of infinite L the spectrum becomes continuous. This spectrum is independent of the force.

Appendix A.2. Single kink (k), uniform force

For a single kink in a polymer of length L with uniform force we choose the origin $x = 0$ as in Section 3 such that we have one crossing point $z_k(0) = 0$ and the end points are at $x = \pm L/2$. We define $-L/2 < x < 0$, where $z_k(x) < 0$ as region I and $0 < x < L/2$, where $z_k(x) > 0$ as region II. In regions I and II we define functions $f_{\mathrm{I}}(x)$ and $f_{\mathrm{II}}(x)$ according to (A.4) or (A.6) with 8 expansion coefficients $C_{\mathrm{I},i}$ and $C_{\mathrm{II},i}$ $(i = 1,\ldots,4)$.

The boundary conditions for fluctuations are $f(\pm L/2) = 0$ and $f'(\pm L/2) = 0$. The kink crosses the barrier in $x = 0$. Continuity requirements give 3 matching conditions $f_{\mathrm{I}}^{(m)}(0) = f_{\mathrm{II}}^{(m)}(0)$ for $m = 0,1,2$. From the δ-function contributions in (A.2) at $x = 0$, one finds the matching condition for the discontinuities of $f'''(x)$. This gives the additional condition

$f'''_{\rm II}(0) - f'''_{\rm I}(0) = 2aV_0 f(0)/\kappa|\partial_x z_k(0)|$. The 8 boundary and matching conditions lead to a homogeneous linear system of equations for the 8 coefficients $C_{{\rm I},i}$ and $C_{{\rm II},i}$. Eigenvalues of equation (A.3) are found from the condition that the determinant of this homogeneous linear system of equations has to be zero.

For solutions of the form (A.6) with $\omega \le V_0/\gamma$, this leads to a condition

$$\sin(K_+L/2) - \sinh(K_+L/2) = 0 \quad \text{or} \tag{A.11}$$

$$\cos(K_+L/2) + \cosh(K_+L/2) - 2 = w_k^3 K_+^3 \left[\sin(K_+L/2) + \sinh(K_+L/2)\right] , \tag{A.12}$$

where we can use $|\partial_x z_k(x)|_{x=0} = a/w_k$. Equations (A.11) and (A.12) have a solution $K_+ = 0$ corresponding to $\omega_{k,1} = V_0/\gamma$. In the limit $L \gg w_k$, there is one more solutions of equation (A.12), $K_+ \approx 1/w_k$, corresponding to a zero mode $\omega_{k,0} = 0$ for the translation of the kink with $f_0 \sim \partial_x z_k$.

For solutions of the form (A.4) with $\omega \ge V_0/\gamma$, we find a condition

$$\tanh(K_-L/2) - \tan(K_-L/2) = 0 \quad \text{or} \tag{A.13}$$

$$1 - \cos(K_-L/2)\cosh(K_-L/2) = w_k^3 K_-^3 \big[\cosh(K_-L/2)\sin(K_-L/2) + \sinh(K_-L/2)\cos(K_-L/2)\big] . \tag{A.14}$$

Obviously roots coming from (A.13) are identical to solutions of (A.8) for a straight configuration of the same length L. This leads to the identification $\omega_{k,p}(L) = \omega_{s,p-1}(L)$ for even $p \ge 2$. In the limit of large K_-L, also the remaining solutions for odd $p \ge 3$ coming from (A.14) have approximately the same spacing as for a straight configuration, *i.e.*, $K_-L \approx b_k + p\pi$ where b_k is a weakly p-dependent constant. For large $p \gg L/w_k$, the roots coming from (A.14) are identical to solutions of (A.9) for a straight configuration such that b_k approaches $b_k \approx -\pi/2$ for large $p \gg L/w_k$.

Finally, we obtain a spectrum

$$\begin{aligned}
&\omega_{k,0} = 0 ,\\
&\omega_{k,1} = V_0/\gamma ,\\
&\omega_{k,p} = \omega_{s,p-1}\\
&\quad \approx V_0/\gamma + \kappa\Big[\Big(-\frac{\pi}{2} + (p-1)\pi\Big)/L\Big]^4 , \text{ for } p \ge 2, \text{ even}\\
&\omega_{k,p} \approx V_0/\gamma + \kappa\left[(b_k + (p-1)\pi)/L\right]^4 , \quad \text{for } p \ge 3, \text{ odd} .
\end{aligned} \tag{A.15}$$

The exact value of b_k becomes irrelevant for large mode numbers p. In the limit of infinite L the spectrum is mixed. We obtain two discrete zero translational modes and a continuum of stable modes with $\omega \ge V_0/\gamma$.

Appendix A.3. Critical nucleus (n), uniform force

For the critical nucleus at uniform force we choose the origin $x = 0$ as in Section 9.1 such that the crossing points are $z_n(0) = 0$ and $z_n(L') = 0$ and the end points are at $x = -L/2$ and $x = L/2 + L'$; this configuration has a total length $L + L'$, where L' is given by (55) as a function of F. With two crossing points we introduce a piecewise definition with three regions. We define region I as $-L/2 < x < 0$ with $z_n(x) < 0$, region II as $0 < x < L'$ with $z_n(x) > 0$, and region III as $L' < x < L/2 + L'$ with $z_n(x) < 0$. In each region we define the functions $f_{\rm I}(x)$, $f_{\rm II}(x)$, and $f_{\rm III}(x)$ according to (A.4) or (A.6) with twelve expansion coefficients $C_{{\rm I},i}$, $C_{{\rm II},i}$, and $C_{{\rm III},i}$ ($i = 1, \ldots, 4$).

The boundary conditions are $f(-L/2) = f(L/2 + L') = 0$ and $f'(-L/2) = f'(L/2 + L') = 0$ for a polymer of length $L + L'$. The critical nucleus crosses the barrier in the two points $x = 0$ and $x = L'$. Continuity requirements give six matching conditions $f_{\rm I}^{(m)}(0) = f_{\rm II}^{(m)}(0)$ and $f_{\rm II}^{(m)}(L') = f_{\rm III}^{(m)}(L')$ for $m = 0, 1, 2$. From the δ-function contributions in (A.2) at $x = 0$ and $x = L'$, one finds the matching condition for the discontinuities of $f'''(x)$. This gives two additional matching conditions $f'''_{\rm II}(0) - f'''_{\rm I}(0) = 2aV_0 f(0)/\kappa|\partial_x z_n(0)|$ and $f'''_{\rm III}(L') - f'''_{\rm II}(L') = 2aV_0 f(L')/\kappa|\partial_x z_n(L')|$. The 12 boundary and matching conditions lead to a homogeneous linear system of equations for the 12 coefficients $C_{{\rm I},i}$, $C_{{\rm II},i}$, and $C_{{\rm III},i}$. Eigenvalues of equation (A.3) are found from the condition that the determinant of this homogeneous linear system of equations has to be zero.

For solutions of the form (A.6) with $\omega \le V_0/\gamma$ and in the limit $K_+L \gg 1$, this leads to a condition

$$\exp(-2K_+L')(1 + \sin(2K_+L')) = \left(K_+^3 w_k^3 \frac{w_k|\partial_x z_n|_{x=0}|}{a} - 1\right)^2 , \tag{A.16}$$

where $\partial_x z_n|_{x=0}$ is given by

$$\begin{aligned}
\frac{w_k \partial_x z_n|_{x=0}}{a} &= 1 - \exp(-\bar{L}') - \frac{F}{F_c}\frac{2\sin(\bar{L}'/2)}{\cos(\bar{L}'/2) + \sin(\bar{L}'/2)}\\
&= 1 - \exp(-\bar{L}')\left(1 + \sin 2\bar{L}'\right)^{1/2}
\end{aligned} \tag{A.17}$$

with $\bar{L}' \equiv L'/w_k$ and where in the last line L' is given by (55) as a function of F. Equation (A.16) gives one unstable mode with negative eigenvalue $\omega_{n,0} < 0$, which corresponds a symmetric mode, a zero translational mode $\omega_{n,1} = 0$, which is asymmetric, and one positive eigenvalue $\omega_{n,2} = V_0/\gamma$. For forces F close to the critical value F_c, we find that the unstable mode has an eigenvalue

$$\omega_{n,0} \approx \frac{V_0}{\gamma}\left[1 - 2^{4/3}\left(1 - \frac{F}{F_c}\right)^{-8/3}\right] . \tag{A.18}$$

For small forces $F \ll F_c$, we find

$$\omega_{n,0} \approx -\frac{16}{3}\frac{V_0}{\gamma}\frac{F}{F_c} , \tag{A.19}$$

and the unstable mode approaches a second zero mode at $F \approx 0$, a "breathing mode" of the resulting kink-antikink pair. In addition to these modes, there exists a set of positive modes corresponding to solutions of the form (A.4) for $\omega > V_0/\gamma$.

Finally, this gives a spectrum

$$\begin{aligned}
&\omega_{n,0} < 0,\\
&\omega_{n,1} = 0,\\
&\omega_{n,2} = V_0/\gamma,\\
&\omega_{k,p} = V_0/\gamma + \left[(b_n + (p-2)\pi)/(L+L')\right]^4 \kappa, \quad \text{for} \quad p \geq 3,
\end{aligned} \tag{A.20}$$

where b_n is a constant that becomes irrelevant for large p. Note that $L+L' \approx L$ for large forces F close to F_c and that $L+L' \approx 2L$ for small forces $F \ll F_c$. In the limit of infinite L the spectrum is mixed. There are two discrete modes, the unstable mode $p = 0$, the zero translational mode $p = 1$ and a continuum of stable modes with $\omega \geq V_0/\gamma$.

References

1. H.A. Kramers, Physica (Utrecht) **7**, 284 (1940).
2. G. Bell, Science **200**, 618 (1978).
3. P. Hänggi, P. Talkner, M. Borkovec, Rev. Mod. Phys. **62**, 251 (1990).
4. J.P. Hirth, J. Lothe, *Theory of Dislocations* (McGraw-Hill, New York, 1968).
5. A Seeger, P. Schiller, in *Physical Acoustics*, edited by W. P. Mason, Vol. **III** (Academic, New York, 1966) p. 361.
6. A.P. Kazantsev, V.L. Pokroskii, Sov. Phys. JETP **31**, 362 (1970) (Zh. Eksp. Teor. Fiz. **58**, 677 (1970)).
7. B.V. Petukhov, V.L. Pokrovskii, Sov, Phys. JETP **36**, 226 (1973) (Zh. Eksp. Teor. Fiz. **63**, 634 (1972)).
8. G. Blatter *et al.*, Rev. Mod. Phys. **66**, 1125 (1994).
9. M.J. Rice, A.R. Bishop, J.A. Krumhansl, S.E. Trullinger, Phys. Rev. B **36**, 432 (1976).
10. M. Büttiker, R. Landauer, Phys. Rev. Lett. **43**, 1453 (1979).
11. J.F. Currie, J.A. Krumhansl, A.R. Bishop, S.E. Trullinger, Phys. Rev. B **22**, 477 (1980).
12. K.L. Sebastian, Phys. Rev. E **61**, 3245 (2000); K.L. Sebastian, Alok K. R. Paul, Phys. Rev. E **62**, 927 (2000).
13. D.K. Lubensky, D.R. Nelson, Biophys. J. **77**, 1824 (1999).
14. W.H. Taylor, P.J. Hagerman, J. Mol. Biol. **212**, 363 (1990).
15. F. Gittes, B. Mickey, J. Nettleton, J. Howard, J. Cell. Biol. **120**, 923 (1993).
16. J. Käs, H. Strey, E. Sackmann, Nature, **368**, 226 (1994).
17. R.N. Netz, J.-F. Joanny, Macromolecules **32**, 9013 (1999).
18. G. Gompper, T.W. Burkhardt, Phys. Rev. A **40**, 6124 (1989).
19. J. Kierfeld, R. Lipowsky, Europhys. Lett. **62**, 285 (2003).
20. J.P. Rabe, S. Buchholz, Science **253**, 424 (1991).
21. S. Cincotti, J.P. Rabe, Appl. Phys. Lett. **62**, 3531 (1993).
22. D.G. Kurth, N. Severin, J.P. Rabe, Angew. Chem. **114**, 3833 (2002); D.G. Kurth, private communication.
23. N. Severin, J. Barner, A.A. Kalachev, J.P. Rabe, NanoLett. **4**, 577 (2004).
24. J. Han, S.W. Turner, H.G. Craighead, Phys. Rev. Lett. **83**, 1688 (1999).
25. T. Pfohl, S. Herminghaus, Phys. J. **2**(1), 35 (2003); S. Köster, Diploma thesis, Ulm University.
26. G. Costantini, F. Marchesoni, Phys. Rev. Lett. **87**, 114102 (2001).
27. P. Kraikivski, R. Lipowsky, J. Kierfeld, Europhys. Lett. **66**, 763 (2004).
28. U. Seifert, W. Wintz, P. Nelson, Phys. Rev. Lett. **77**, 5389 (1996)
29. R. Everaers, F. Jülicher, A. Ajdari, A.C. Maggs, Phys. Rev. Lett. **82**, 3717 (1999).
30. A. Ajdari, F. Jülicher, A. Maggs, J. Phys. I **7**, 823 (1997).
31. T.B. Liverpool, A.C. Maggs, Macromolecules **34**, 6064 (2001).
32. O. Hallatschek, E. Frey, K. Kroy, Phys. Rev. E **70**, 031802 (2004).
33. Note the different convention compared to reference [27], where we set $r = 1$.
34. N.G. van Kampen, *Stochastic Processes in Physics and Chemistry* (Elsevier Science, Amsterdam, 1992).
35. P. Hänggi, F. Marchesoni, P. Sodano, Phys. Rev. Lett. **60**, 2563 (1988).
36. M. Doi, S.F. Edwards, *The Theory of Polymer Dynamics* (Clarendon, Oxford, 1986).
37. A. Ashkin, Science **210**, 1081 (1980).
38. T.R. Strick *et al.*, Science **271**, 1835 (1996).
39. P. Kraikivski, R. Lipowsky, J. Kierfeld, to be published.